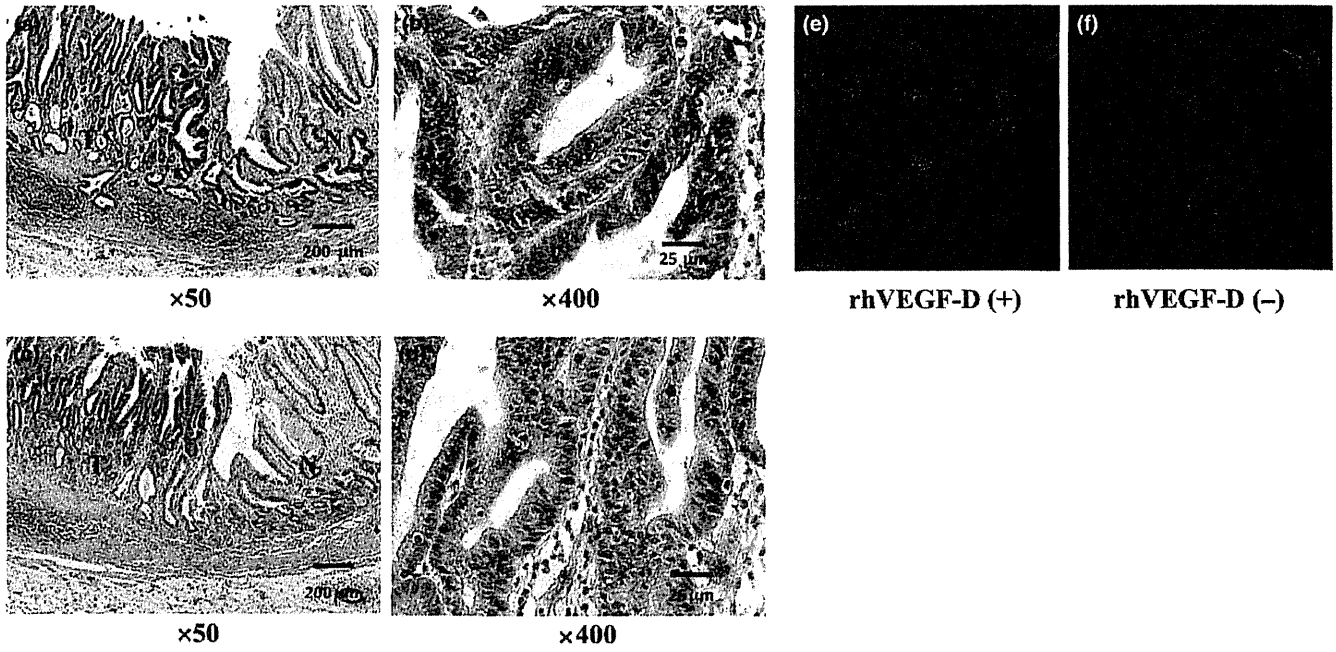

Fig. 1. Immunohistochemical staining for (a,b) VEGF-D and (c,d) VEGFR-3 in human gastric carcinoma tissues. Immunoreactivities for VEGF-D and VEGFR-3 were detected in tumor cells (T) but not in normal gastric mucosa (N). Scale bars: (a,c) 200 μm, (b,d) 25 μm. Immunofluorescence staining for phosphorylation of VEGFR-3 after stimulation with (e) or without (f) VEGF-D in KKLS cells. Tumor cells stained positively for pVEGFR-2,3 (red).

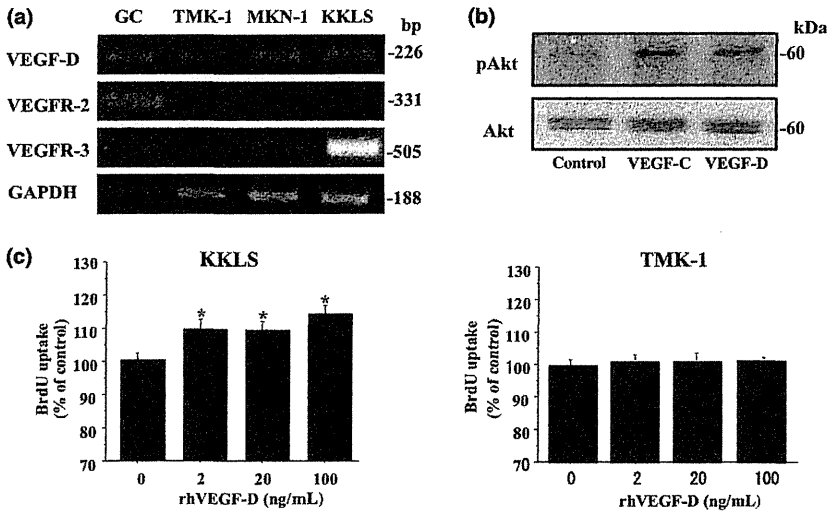

Fig. 2. Expression of VEGF-D, VEGFR-2, and VEGFR-3 in gastric carcinoma cell lines and effect of VEGF-D on KKLS cells. (a) VEGF-D, VEGFR-2, and VEGFR-3 expression by gastric carcinoma cell lines was examined by RT-PCR. Gastric cancer tissue (GC) was used for control. (b) Western blot for phosphorylation of Akt. Treatment with VEGF-C or VEGF-D induced Ser473 phosphorylation of Akt in KKLS cells. (c) KKLS and TMK-1 cells were incubated with rhVEGF-D (2, 20, or 100 ng/mL) for 24 h, and cell proliferation was measured with a cell proliferation ELISA system. $*P < 0.05$; bars, SE.

KKLS cells to grow *in vitro* was evaluated. Transfection with VEGF-D increased *in vitro* cell growth of KKLS cells (Fig. 4c). To examine the effect of VEGF-D overexpression in an animal model, we transplanted KKLS/VEGF-D and KKLS/mock cells into the gastric wall of nude mice. The mice were killed after 4 weeks, and tumors derived from KKLS/VEGF-D cells were significantly larger than KKLS/mock tumors (Fig. 4d). VEGF-D secreted by the tumor did not promote lymphatic metastasis.

Immunohistochemistry for Ki-67, CD31, and Lyve1 and *in situ* detection of apoptotic cells in KKLS cells growing in the gastric wall of nude mice. We evaluated MVD, LVD, and the Ki-67 labeling index based on immunodetection of CD31, Lyve1, and Ki-67. Indeed, statistically significant increases in MVD (Fig. 5a) and the Ki-67 labeling index (Fig. 5b) were noted in KKLS/VEGF-D tumors in comparison to those in KKLS/mock tumors. The number of lymphatic vessels was not increased in response to VEGF-D transfection (data not shown); however, the luminal area of lymphatic vessels was significantly enlarged (Fig. 5c). The apoptotic index was also evaluated. A significant decrease in the apoptotic index was noted in KKLS/VEGF-D tumors in comparison to that in KKLS/mock tumors (Fig. 5d).

Discussion

VEGF-C and VEGF-D are specific ligands for VEGFR-3 and VEGFR-2.[27,28] They have been shown to stimulate lymphangiogenesis and angiogenesis both *in vitro* and *in vivo*.[10–23] It has been reported that VEGF-D induced lymphangiogenesis in a mouse tumor model.[10,29] The expression of VEGF-D has

doi: 10.1111/j.1349-7006.2010.01649.x

Table 2. cDNA microarray analysis of KKLS cells treated with VEGF-D

Gene function	Gene symbol	Gene name	Fold change*
Cell cycle regulator	CCND1	Cyclin D1	3
	CDK4	Cyclin-dependent kinase 4	2.8
Apoptosis	BCL2	B-cell CLL/lymphoma 2	6.3
	DAPK2	Death-associated protein kinase 1	5.9
	NDUFA13	Cell death-regulatory protein GRIM19	2.8
Angiogenesis	THBS1	Thrombospondin 1	7.3
	ANG	Angiogenin, ribonuclease, RNase A family, 5	4.2
Cell adhesion	CDH1	Cadherin 1, type 1, E-cadherin (epithelial)	5.1
	ITGA7	Integrin, alpha 7	3.8
	CTNNA2	Catenin (cadherin-associated protein), alpha 2	3.6
	VIM	Vimentin	3.3
Motility, invasion	PLG	Plasminogen	10.8
	PLAUR	Plasminogen activator, urokinase receptor	4
	AMFR	Autocrine motility factor receptor	2.9

*Fold change = the degree of upregulation in comparison to expression in control (untreated) cells.

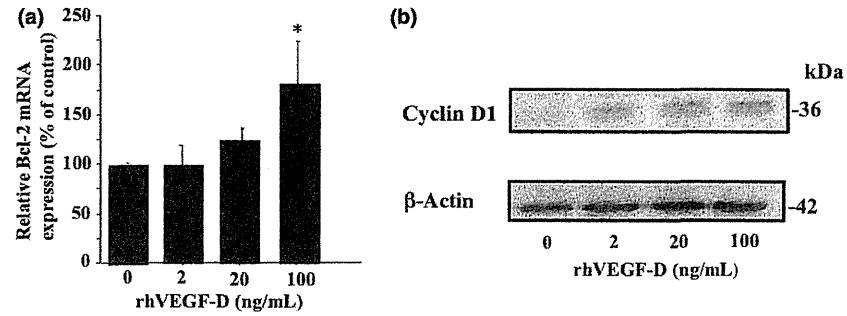

Fig. 3. KKLS cells were treated with rhVEGF-D (2, 20, or 100 ng/mL) for 8 h. Expression of (a) Bcl-2 and (b) cyclin D1 was examined by real-time PCR and western blot analysis, respectively. PCR were carried out in triplicate. Data for real-time PCR were normalized to those of β-actin. $*P < 0.05$; bars, SE.

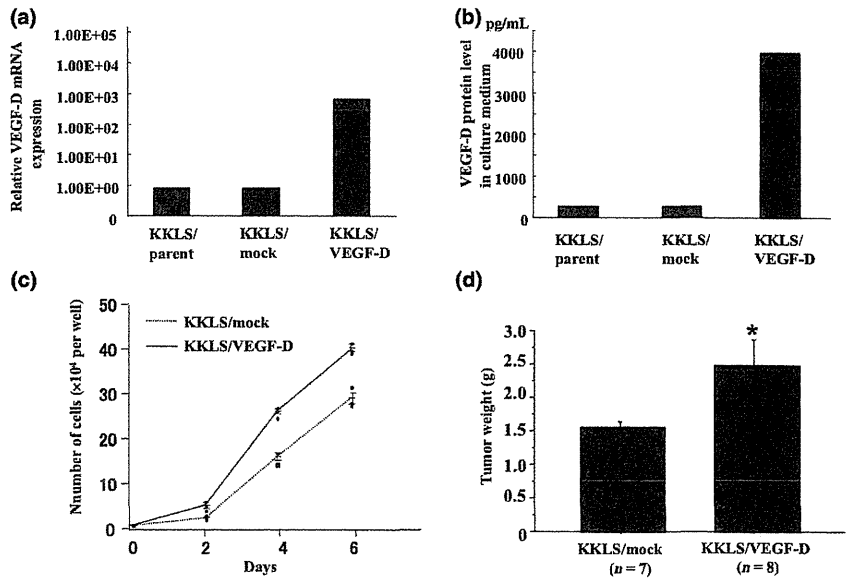

Fig. 4. Establishment of clonal cell line overexpressing VEGF-D, and *in vitro* and *in vivo* growth of VEGF-D-transfected cells. (a) Expression of VEGF-D mRNA was examined by real-time PCR. (b) VEGF-D protein level in culture medium was examined by ELISA. (c) *In vitro* cell growth of VEGF-D-transfected KKLS cells. Cells (1×10^4) were seeded in a six-well plate and cultured in RPMI-1640 containing 0.5% FBS. The number of cells was determined in triplicate cultures. (d) Orthotopic (gastric mucosa) xenograft model. Tumor weight at 4 weeks after transplantation of the VEGF-D-overexpressing clone (KKLS/VEGF-D) and corresponding vector control (KKLS/control). $*P < 0.05$; bars, SE.

been correlated with tumor lymphangiogenesis and lymph node metastasis in many human carcinomas, including breast,[14] lung,[19] gastric,[18] and colorectal cancers.[13] We previously examined expression of VEGF-C and VEGF-D by immunohistochemistry in 140 archival surgical specimens of submucosally invasive gastric carcinoma. VEGF-C immunoreactivity was associated with histologic type, lymphatic invasion, lymph node metastasis, and MVD. There was no association between VEGF-D immunoreactivity and clinicopathologic features. These results suggest that VEGF-C is the dominant regulator of lymphangiogenesis in early stage human gastric carcinoma.[22]

VEGFR-3 has also been detected in several types of malignant cells,[30,31] although it is mainly expressed by lymphatic endothelial cells. In various types of cancer cells, autocrine VEGF-A/VEGFR-2 loops on tumor cells regulate their growth and survival.[32–34] We and others have reported the existence of autocrine stimulation of tumor growth via the VEGF-C/VEG-

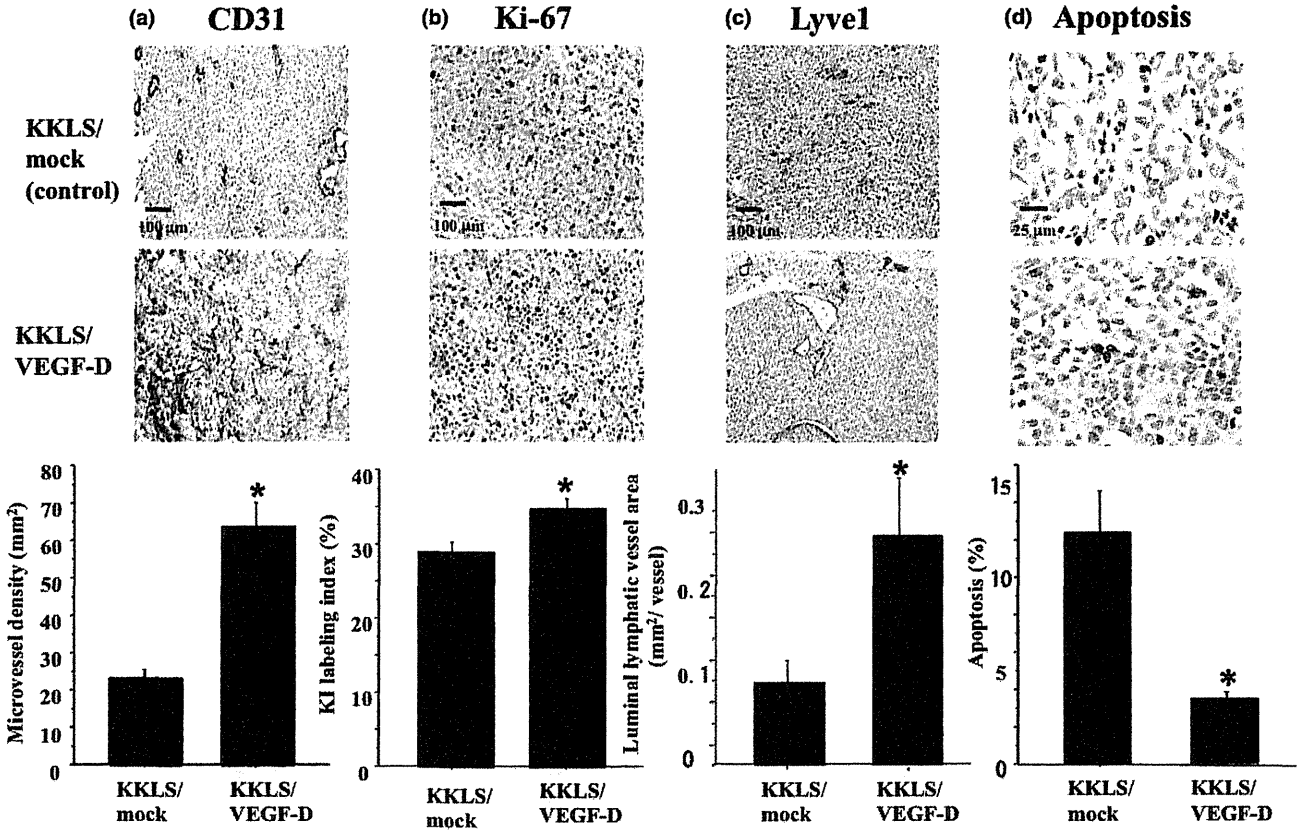

Fig. 5. Immunohistochemistry for (a) CD31, (b) Ki-67, and (c) Lyve1, and (d) *in situ* detection of apoptotic cells in KKLS cells growing in the gastric wall of nude mice. Lower panels, quantification of CD31-positive vessels, Ki-67-positive cells, Lyve1-positive vessels, and apoptotic cells. Scale bars: (a,c) 200 μm. *$P < 0.05$; bars, SE.

FR-3 axis in lung,[30] breast,[31] and gastric cancers.[24] In the present study, we examined the expression of VEGF-D and VEGFR-3 in human gastric carcinomas and the role of the VEGF-D/VEGFR-3 axis in tumor cells. In 10 of 29 (34%) gastric carcinoma specimens, tumor cells expressed both VEGF-D and VEGFR-3. Treatment of KKLS cells (VEGFR-3-expressing cell line) with recombinant VEGF-D induced tyrosine phosphorylation of VEGFR-3 and Akt, indicating that VEGFR-3 on tumor cells is functional. Microarray analysis showed up-regulation of cyclin D1 (cell cycle regulator) and Bcl-2 (anti-apoptotic protein) by treatment with VEGF-D. We reported previously that treatment with VEGF-C induced phosphorylation of VEGFR-3 and Akt and increased expression of cyclin D1, PlGF, autocrine motility factor (AMF), and AMF receptor by KKLS cells.[24] Makinen *et al.*[35] showed that VEGFR-3 signaling induces protein kinase C (PKC)-dependent p42/p44 MAPK activation and wortmannin-sensitive phosphorylation of Akt. These findings suggest that VEGF-C and VEGF-D are associated with cell proliferation and survival via these signaling cascades in tumor cells.

To stimulate VEGF-D/VEGFR-3 signaling in an autocrine manner, VEGF-D expression vector was transfected into KKLS cells (KKLS/VEGF-D cells), and these cells were then transplanted into the gastric wall of nude mice. It has been reported that binding of VEGF-D to VEGFR-3 on the lymphatic endothelial cells resulted in dilatation of existing lymphatic vessels as well as in vegetation of new vessels.[36] In the present study, the luminal area of lymphatic vessels was increased in KKLS/VEGF-D tumors in comparison to that in control (KKLS/mock) tumors, indicating that the KKLS/VEGF-D cells produce functional VEGF-D protein. However, VEGF-D secreted by the tumor did not promote lymphatic metastasis. In contrast, Stacker *et al.*[10] reported that expression of VEGF-D in tumor cells led to spread of the tumor to lymph nodes. These discrepancies may be due to differences in cell lines and experimental animal models. Lymphatic metastasis is the consequence of a complex metastatic process, which includes lymphangiogenesis,[37,38] dissemination, transport, settlement, and growth in the lymphatic system. These involve not only VEGF-D but many other growth factors such as VEGF-C, angiopoietins, fibroblast growth factor, and platelet-derived growth factor.[39]

In vitro treatment with VEGF-D increased expression of cyclin D1 and stimulated proliferation of KKLS cells. The Ki-67 labeling index and tumor weight increased in orthotopic KKLS/VEGF-D tumors in comparison to those in orthotopic KKLS/mock tumors. These increases were associated with increased MVD, indicating that VEGF-D transfection into KKLS cells stimulates angiogenesis. In addition, we found that *in vitro* treatment with VEGF-D increased expression of Bcl-2, a key regulator of apoptotic inhibition. The number of apoptosis cells was lower in KKLS/VEGF-D tumors than in KKLS/mock tumors. Consistent with our results, Akahane *et al.*[40] reported that overexpression of VEGF-D in breast cancer cell lines resulted in up-regulation of the *Bcl-2* gene.

In conclusion, human gastric carcinoma cells express VEGF-D as well as VEGFR-3. VEGF-D may be involved in the progression of human gastric carcinoma not only by stimulating angiogenesis and lymphangiogenesis via a paracrine mechanism, but also by regulating cell proliferation and apoptosis via an autocrine mechanism. Further studies are needed to identify precise signaling mechanisms responsible for the autocrine role of VEGF-D.

doi: 10.1111/j.1349-7006.2010.01649.x

Acknowledgments

This work was carried out with the kind cooperation of the Analysis Center of Life Science, Hiroshima University (Hiroshima, Japan) and was supported, in part, by Grants-in-Aid for Cancer Research from the Ministry of Education, Culture, Science, Sports and Technology of Japan, and from the Ministry of Health, Labor and Welfare of Japan.

Disclosure Statement

The authors have no conflict of interest.

References

1 Smith MG, Hold GL, Tahara E, El-Omar EM. Cellular and molecular aspects of gastric cancer. *World J Gastroenterol* 2006; **12**: 2979–90.
2 Stacker SA, Achen MG, Jussila L, Baldwin ME, Alitalo K. Lymphangiogenesis and cancer metastasis. *Nat Rev Cancer* 2002; **2**: 573–83.
3 Ferrara N. VEGF and the quest for tumour angiogenesis factors. *Nat Rev Cancer* 2002; **2**: 795–803.
4 Alitalo K, Carmeliet P. Molecular mechanisms of lymphangiogenesis in health and disease. *Cancer Cell* 2002; **1**: 219–27.
5 Berse B, Brown LF, Van de Water L, Dvorak HF, Senger DR. Vascular permeability factor (vascular endothelial growth factor) gene is expressed differentially in normal tissues, macrophages, and tumors. *Mol Biol Cell* 1992; **3**: 211–20.
6 Ferrara N, Houck K, Jakeman L, Leung DW. Molecular and biological properties of the vascular endothelial growth factor family of proteins. *Endocr Rev* 1992; **13**: 18–32.
7 Otrock ZK, Makarem JA, Shamseddine AI. Vascular endothelial growth factor family of ligands and receptors: review. *Blood Cells Mol Dis* 2007; **38**: 258–68.
8 Orlandini M, Marconcini L, Ferruzzi R, Oliviero S. Identification of a c-fos-induced gene that is related to the platelet-derived growth factor/vascular endothelial growth factor family. *Proc Natl Acad Sci USA* 1996; **93**: 11675–80.
9 Stacker SA, Stenvers K, Caesar C *et al.* Biosynthesis of vascular endothelial growth factor-D involves proteolytic processing which generates non-covalent homodimers. *J Biol Chem* 1996; **274**: 32127–36.
10 Stacker SA, Caesar C, Baldwin ME *et al.* VEGF-D promotes the metastatic spread of tumor cells via the lymphatics. *Nat Med* 2001; **7**: 186–91.
11 Thelen A, Scholz A, Benckert C *et al.* VEGF-D promotes tumor growth and lymphatic spread in a mouse model of hepatocellular carcinoma. *Int J Cancer* 2008; **122**: 2471–81.
12 Von Marschall Z, Scholz A, Stacker SA *et al.* Vascular endothelial growth factor-D induces lymphangiogenesis and lymphatic metastasis in models of ductal pancreatic cancer. *Int J Oncol* 2005; **27**: 669–79.
13 White JD, Hewett PW, Kosuge D *et al.* Vascular endothelial growth factor-D expression is an independent prognostic marker for survival in colorectal carcinoma. *Cancer Res* 2002; **62**: 1669–75.
14 Nakamura Y, Yasuoka H, Tsujimoto M *et al.* Prognostic significance of vascular endothelial growth factor D in breast carcinoma with long-term follow-up. *Clin Cancer Res* 2003; **9**: 716–21.
15 Kurahara H, Takao S, Maemura K, Shinchi H, Natsugoe S, Aikou T. Impact of vascular endothelial growth factor-C and -D expression in human pancreatic cancer: its relationship to lymph node metastasis. *Clin Cancer Res* 2004; **10**: 8413–20.
16 Yokoyama Y, Charnock-Jones DS, Licence D *et al.* Vascular endothelial growth factor-D is an independent prognostic factor in epithelial ovarian carcinoma. *Br J Cancer* 2003; **88**: 237–44.
17 Yokoyama Y, Charnock-Jones DS, Licence D *et al.* Expression of vascular endothelial growth factor (VEGF)-D and its receptor, VEGF receptor 3, as a prognostic factor in endometrial carcinoma. *Clin Cancer Res* 2003; **9**: 1361–9.
18 Jüttner S, Wissmann C, Jöns T *et al.* Vascular endothelial growth factor-D and its receptor VEGFR-3: two novel independent prognostic markers in gastric adenocarcinoma. *J Clin Oncol* 2006; **24**: 228–40.
19 Niki T, Iba S, Tokunou M, Yamada T, Matsuno Y, Hirohashi S. Expression of vascular endothelial growth factors A, B, C, and D and their relationships to lymph node status in lung adenocarcinoma. *Clin Cancer Res* 2000; **6**: 2431–9.
20 O-charoenrat P, Rhys-Evans P, Eccles SA. Expression of vascular endothelial growth factor family members in head and neck squamous cell carcinoma correlates with lymph node metastasis. *Cancer* 2001; **92**: 556–68.
21 George ML, Tutton MG, Janssen F *et al.* VEGF-A, VEGF-C, and VEGF-D in colorectal cancer progression. *Neoplasia* 2001; **3**: 420–7.
22 Onogawa S, Kitadai Y, Tanaka S, Kuwai T, Kimura S, Chayama K. Expression of VEGF-C and VEGF-D at the invasive edge correlates with lymph node metastasis and prognosis of patients with colorectal carcinoma. *Cancer Sci* 2004; **95**: 32–9.
23 Kitadai Y, Kodama M, Cho S *et al.* Quantitative analysis of lymphangiogenic markers for predicting metastasis of human gastric carcinoma to lymph nodes. *Int J Cancer* 2005; **115**: 388–92.
24 Kodama M, Kitadai Y, Tanaka M *et al.* Vascular endothelial growth factor C stimulates progression of human gastric cancer via both autocrine and paracrine mechanism. *Clin Cancer Res* 2008; **14**: 7205–14.
25 Japanese Research Society for Gastric Cancer. *Japanese Classification of Gastric Carcinoma.* Kanehara & Co., Tokyo, 1999.
26 Weidner N, Semple JP, Welch WR, Folkman J. Tumor angiogenesis and metastasis: correlation in invasive breast carcinoma. *N Engl J Med* 1991; **324**: 1–8.
27 Joukov V, Pajusola K, Kaipainen A *et al.* A novel vascular endothelial growth factor, VEGF-C, is a ligand for the Flt4 (VEGFR-3) and KDR (VEGFR-2) receptor tyrosine kinases. *EMBO J* 1996; **15**: 290–8.
28 Achen MG, Jeltsch M, Kukk E *et al.* Vascular endothelial growth factor D (VEGF-D) is a ligand for the tyrosine kinases VEGF receptor 2 (Flk1) and VEGF receptor 3 (Flt4). *Proc Natl Acad Sci USA* 1998; **95**: 548–53.
29 Kopfstein L, Veikkola T, Djonov VG *et al.* Distinct roles of vascular endothelial growth factor-D in lymphangiogenesis and metastasis. *Am J Pathol* 2007; **170**: 1348–61.
30 Tanno S, Ohsaki Y, Nakanishi K, Toyoshima E, Kikuchi K. Human small cell lung cancer cells express functional VEGF receptors, VEGFR-2 and VEGFR-3. *Lung Cancer* 2004; **46**: 11–19.
31 Timoshenko AV, Rastogi S, Lala PK. Migration-promoting role of VEGF-C and VEGF-C binding receptors in human breast cancer cells. *Br J Cancer* 2007; **97**: 1090–8.
32 Von Marschall Z, Cramer T, Höcker M *et al.* De novo expression of vascular endothelial growth factor in human pancreatic cancer: evidence for an autocrine mitogenic loop. *Gastroenterology* 2000; **119**: 1358–72.
33 Bachelder RE, Wendt MA, Mercurio AM. Vascular endothelial growth factor promotes breast carcinoma invasion in an autocrine manner by regulating the chemokine receptor CXCR4. *Cancer Res* 2002; **62**: 7203–6.
34 Jackson MW, Roberts JS, Heckford SE *et al.* A potential autocrine role for vascular endothelial growth factor in prostate cancer. *Cancer Res* 2002; **62**: 854–9.
35 Mäkinen T, Veikkola T, Mustjoki S *et al.* Isolated lymphatic endothelial cells transduce growth, survival and migratory signals via the VEGF-C/D receptor VEGFR-3. *EMBO J* 2002; **20**: 4762–73.
36 Veikkola T, Jussila L, Makinen T *et al.* Signalling via vascular endothelial growth factor receptor-3 is sufficient for lymphangiogenesis in transgenic mice. *EMBO J* 2001; **20**: 1223–31.
37 Achen MG, McColl BK, Stacker SA. Focus on lymphangiogenesis in tumor metastasis. *Cancer Cell* 2005; **7**: 121–7.
38 Karpanen T, Alitalo K. Lymphatic vessels as targets of tumor therapy? *J Exp Med* 2001; **194**: F37–42.
39 Folkman J. Looking for a good endothelial address. *Cancer Cell* 2002; **1**: 113–15.
40 Akahane M, Akahane T, Matheny SL, Shah A, Okajima E, Thorgeirsson UP. Vascular endothelial growth factor-D is a survival factor for human breast carcinoma cells. *Int J Cancer* 2006; **118**: 841–9.

Expression of platelet-derived growth factor (PDGF)-B and PDGF-receptor β is associated with lymphatic metastasis in human gastric carcinoma

Michiyo Kodama,[1] Yasuhiko Kitadai,[1,4] Tomonori Sumida,[1] Mayu Ohnishi,[1] Eiji Ohara,[1] Miwako Tanaka,[1] Kei Shinagawa,[1] Shinji Tanaka,[2] Wataru Yasui[3] and Kazuaki Chayama[1]

[1]Department of Medicine and Molecular Science, Hiroshima University Graduate School of Biomedical Sciences, Hiroshima; [2]Department of Endoscopy, Hiroshima University Hospital, Hiroshima; [3]Department of Pathology, Hiroshima University Graduate School of Biomedical Sciences, Hiroshima, Japan

(Received March 15, 2010/Revised May 25, 2010/Accepted May 28, 2010/Accepted manuscript online June 7, 2010/Article first published online July 7, 2010)

Recent study of murine fibrosarcoma has revealed that platelet-derived growth factor (PDGF) plays a direct role in promoting lymphangiogenesis and metastatic spread to lymph nodes. Thus, we investigated the relation between PDGF and PDGF receptor (PDGF-R) expression and lymphatic metastasis in human gastric carcinoma. We examined PDGF-B and PDGF-Rβ expression in four human gastric carcinoma cell lines (TMK-1, MKN-1, MKN-45, and KKLS) and in 38 surgical specimens of gastric carcinoma. PDGF-B and PDGF-Rβ expression was examined by immunofluorescence in surgical specimens and in human gastric carcinoma cells (TMK-1) implanted orthotopically in nude mice. Groups of mice (n = 10, each) received saline (control) or PDGF-R tyrosine kinase inhibitor imatinib. PDGF-B and PDGF-Rβ mRNA expression was significantly higher in patients with lymph node metastasis than in those without and was also significantly higher in diffuse-type carcinoma than in intestinal-type carcinoma. In surgical specimens, tumor cells expressed PDGF-B, but PDGF-Rβ was expressed predominantly by stromal cells. Under culture conditions, expression of PDGF-B mRNA was found in all of the gastric cell lines, albeit at different levels. In orthotopic TMK-1 tumors, cancer cells expressed PDGF-B but not PDGF-Rβ. PDGF-Rβ was expressed by stromal cells, including lymphatic endothelial cells. Four weeks of treatment with imatinib significantly decreased the area of lymphatic vessels. Our data indicate that secretion of PDGF-B by gastric carcinoma cells and expression of PDGF-Rβ by tumor-associated stromal cells are associated with lymphatic metastasis. Blockade of PDGF-R signaling pathways may inhibit lymph node metastasis of gastric carcinoma. (*Cancer Sci* 2010; 101: 1984–1989)

Gastric cancer is one of the most frequent malignancies in the world. The major cause of mortality is metastasis, which relies on *de novo* formation of blood and lymphatic vessels.[1] Although induction of tumor angiogenesis is known to be a complex process that involves the interplay of a dozen or more tumor-derived growth factors,[2] how tumors induce lymphangiogenesis is poorly understood.

Among known lymphangiogenic factors, the best-characterized growth factors are vascular endothelial growth factor C (VEGF-C) and VEGF-D.[3–8] Fibroblast growth factor-2 promotes lymphatic vessel growth in the mouse cornea, but this effect is believed to occur indirectly, via induction of VEGF-C expression and activation of VEGF receptor 3 (VEGFR-3) signaling.[9] It is unlikely that VEGF-C and -D and VEGFR-3 are the sole factors regulating such processes. A range of lymphangiogenic factors produced by tumor cells, endothelial cells, and stromal cells has recently been identified. These include VEGF-A, and members of the hepatocyte growth factor (HGF) and angiopoietin (Ang) families.[10–12] Additionally, interesting preclinical studies have indicated that platelet-derived growth factors (PDGFs) and PDGF receptors (PDGF-Rs) not only promote hemangiogenesis and direct tumor cell growth but are important players in lymphangiogenesis.[13]

Members of the PDGF family are often expressed at high levels in many malignant tissues.[14] The PDGF family consists of five isoforms, -AA, -AB, -BB, -CC, and -DD, usually referred to as PDGF-A (AA), PDGF-B (AB and BB), PDGF-C (CC), and PDGF-D (DD).[15] Their biological activities are mediated by three forms of the tyrosine kinase receptor encoded by two gene products, PDGF-Rα and -Rβ. PDGF-Rα binds all possible forms of PDGF except PDGF-DD, whereas PDGF-Rβ preferentially binds PDGF-BB.[16] PDGFs have been found to induce tumor growth by directly stimulating growth of certain types of tumor cells,[17] to stimulate angiogenesis,[18] to recruit pericytes[19] and to control the interstitial fluid pressure in stroma, influencing transvascular transport of chemotherapeutic agents in a paracrine manner.[20] Recently, Cao *et al.*[13] showed that expression of PDGF-B in murine fibrosarcoma cells induced tumor lymphangiogenesis, leading to enhanced lymph node metastasis. However, there is no report concerning the relation between PDGF-B and PDGF-Rβ expression and lymphatic metastasis in human gastric carcinoma. Thus, we examined the expression profile of PDGF-B and PDGF-Rβ in human gastric carcinoma, and we examined whether blocking PDGF-R can inhibit lymphangiogenesis of gastric cancer *in vivo*.

Materials and Methods

Patients and tumor specimens. Endoscopic biopsy specimens (tumor and corresponding normal mucosa) of gastric tissue from 38 patients with gastric carcinoma who later underwent surgical resection at Hiroshima University Hospital were snap-frozen in liquid nitrogen and stored at −80°C until RNA extraction for quantitative RT-PCR. Informed consent was obtained from all patients for participation in the study according to the Declaration of Helsinki. Pathology reports and clinical histories were reviewed for accurate staging at the time of surgery. Criteria for staging and histologic classification were those proposed by the Japanese Research Society for Gastric Cancer.[21] Lymph node status was determined by routine pathological examination with the surgical specimens. Two groups of patients, those with lymph node metastasis (node-positive group, n = 21) and those without (node-negative group, n = 17), were closely matched for histologic type and depth of invasion. The patient group comprised 34 men and four women with a median age of

[4]To whom correspondence should be addressed.
E-mail: kitadai@hiroshima-u.ac.jp

doi: 10.1111/j.1349-7006.2010.01639.x

66.5 years. All patients had invasive gastric carcinoma in which the tumor invasion was beyond the submucosa.

Cell cultures. Four cell lines established from human gastric carcinomas and human osteosarcoma cell line MG63 were maintained in RPMI-1640 (Nissui, Tokyo, Japan) with 10% fetal bovine serum (FBS; MA BioProducts, Baltimore, MD, USA). TMK-1 cell line (a poorly differentiated adenocarcinoma) was provided by Dr E. Tahara of Hiroshima University. KKLS cell line (an undifferentiated carcinoma) was provided by Dr Y. Takahashi of Chiba University, Chiba, Japan. Two other cell lines (MKN-1, from an adenosquamous carcinoma, and MKN-45, from a poorly differentiated adenocarcinoma) as well as MG63 were obtained from the Health Science Research Resources Bank, Osaka, Japan.

Quantitative real-time RT-PCR analysis. Total RNA was extracted from gastric carcinoma cell lines and biopsy specimens with an RNeasy Kit (Qiagen, Valencia, CA, USA) according to the manufacturer's instructions. cDNA was synthesized from 1 μg total RNA with a first-strand cDNA synthesis kit (Amersham Biosciences, Piscataway, NJ, USA). After reverse transcription of RNA into cDNA, quantitative RT-PCR was performed with a LightCycler-FastStart DNA Master SYBR-Green I Kit (Roche Diagnostics, Basel, Switzerland) according to the manufacturer's recommended protocol. Polymerase chain reaction (PCR) reactions were carried out in triplicate. To correct for differences in both RNA quality and quantity between samples, values were normalized to those of β-actin. The mRNA ratio between gastric carcinoma tissues (T) and corresponding normal mucosa (N) was calculated and expressed as the T/N ratio. Primers for PCR were designed with specific primer analysis software (Primer Designer; Scientific and Educational Software, Durham, NC, USA), and specificity of the sequences was confirmed by FASTA (EMBL Database). Respective primer sequences, annealing temperatures, and PCR cycles were as follows: PDGF-B forward, CGAGTTGGACCTGAACATGA and PDGF-B reverse, GTCACCGTGGCCTTCTTAAA (PDGF-B PCR product, 339 bp; 58°C; 35 cycles); PDGF-Rβ forward, AGCTACCCCTCAAGGAATCATAG and PDGF-Rβ reverse, CTCTGGTGGATGGATTAAGACTG (PDGF-Rβ PCR product, 376 bp; 58°C; 35 cycles); and GAPDH forward, ATCATCCCTGCCTCTACTGG and GAPDH reverse, CCCTCCGACGCCTGCTTCAC (GAPDH PCR product, 188 bp; 55°C; 28 cycles).

Reagents. Imatinib (imatinib mesylate or Gleevec; Novartis Pharma, Basel, Switzerland) is a 2-phenylaminopyrimidine class protein-tyrosine kinase inhibitor of PDGF-R, BCR–ABL, and c-Kit.[22,23] Imatinib was diluted in sterile water for oral administration. Primary antibodies were purchased from as follows: polyclonal rabbit anti-PDGF-Rβ and polyclonal rabbit anti-PDGF-B subunit from Santa Cruz Biotechnology (Santa Cruz, CA, USA); and rat antimouse Lyve-1 from R&D Systems (Minneapolis, MN, USA).

Western blot analysis. After three washes with cold phosphate-buffered saline (PBS) containing 1 mmol/L sodium orthovanadate, cells were lysed. Proteins (total protein 20 μg) were separated by SDS-PAGE and transferred to nitrocellulose transfer membranes (Whatman, Dassel, Germany). The immune complexes were visualized by enhanced chemiluminescence with an ECL Plus Kit (GE Healthcare, Buckinghamshire, UK).

Animals and orthotopic implantation of tumor cells. Male athymic BALB/c nude mice were obtained from Charles River Japan (Tokyo, Japan). The mice were maintained under specific pathogen-free conditions and used at 5 weeks of age. This study was carried out after permission was granted by the Committee on Animal Experimentation of Hiroshima University.

Subconfluent gastric cancer cells (TMK-1 or KKLS cells) to be used for implantation were harvested by brief treatment with 0.25% trypsin and 0.02% ethylenediamine tetraacetic acid, and then resuspended to a final concentration of 2.0×10^7 cells/mL Hanks' solution. With the use of a 30-gauge needle attached to a 1-mL syringe, cells (1×10^6 cells in 50 μL) were implanted into the gastric walls in the nude mice under observation with a zoom stereomicroscope. After 4 weeks, the mice were killed, and the tumors were resected for study. The tumors were embedded in OCT compound (Miles, Elkhart, IN, USA), rapidly frozen in liquid nitrogen, and stored at −80°C.

Immunofluorescence staining for PDGF-B and PDGF-Rβ, and double staining for PDGF-Rβ and Lyve-1. Fresh frozen specimens of human gastric carcinomas as well as human gastric carcinomas growing in nude mice were cut into 8-μm sections, mounted on positively charged slides, and stored at −80°C. Tissue sections were fixed in cold acetone for 10 min and then washed three times with PBS for 3 min each. Slides were placed in a humidified chamber and incubated with protein blocking solution (5% normal horse serum and 1% normal goat serum in PBS) for 20 min at room temperature. The slides were incubated overnight at 4°C with primary antibody against PDGF-B or PDGF-Rβ, then rinsed three times with PBS, incubated for 10 min in protein blocking solution, and incubated for 1 h at room temperature with Cy3-conjugated goat antirabbit secondary antibody. From this point onwards, the slides were protected from light. The samples were then rinsed three times in PBS. To identify lymph endothelial cells, slides were incubated overnight at 4°C with antibody against Lyve-1. The sections were rinsed three times with PBS and incubated for 10 min in protein blocking solution. Slides were then incubated for 1 h at room temperature with corresponding Cy5-conjugated secondary antibody, and the samples were rinsed three times in PBS. 4′,6-diamidino-2-phenylindole (DAPI) nuclear counterstain was applied for 10 min. Samples were then rinsed three times with PBS, and mounting medium was placed on each sample, which was then covered with a glass coverslip. We used Fluoromount/Plus (Diagnostic Bio Systems, Pleasanton, CA, USA) as the mounting medium.

Confocal microscopy. Confocal fluorescence images were obtained at ×203 or ×403 magnification on a Zeiss LSM 510 laser scanning microscopy system (Carl Zeiss, Thornwood, NY, USA) equipped with a motorized Axioplan microscope, argon laser (458/477/488/514 nm, 30 mW), HeNe lasers (543 nm, 1 mW; 633 nm, 5 mW), LSM 510 control and image acquisition software, and appropriate filters (Chroma Technology, Brattleboro, VT, USA). Confocal images were exported to Adobe Photoshop (Adobe Systems, San Jose, CA, USA), and photo montages were prepared for publication. Lymphatic endothelial cells were identified by green fluorescence, whereas PDGF and PDGF-R were identified by red fluorescence.

Treatment of established human gastric cancer tumors growing in murine gastric walls. Fourteen days after orthotopic

Table 1. Results of quantitative real-time PCR for mRNA expression of PDGF-B and PDGF-Rβ of human gastric carcinoma specimens

	PDGF-Rβ		PDGF-B	
Lymph node status				
Node-positive (n = 21)	6.46 ± 1.45	P = 0.0001	5.06 ± 1.88	P = 0.027
Node-negative (n = 17)	0.97 ± 0.29		0.95 ± 0.18	
Histologic type				
Intestinal (n = 22)	1.32 ± 0.42	P = 0.0041	1.54 ± 0.71	P = 0.028
Diffuse (n = 16)	5.45 ± 1.33		5.02 ± 2.16	

PDGF-B, platelet-derived growth factor B; PDGF-Rβ, PDGF receptor β.

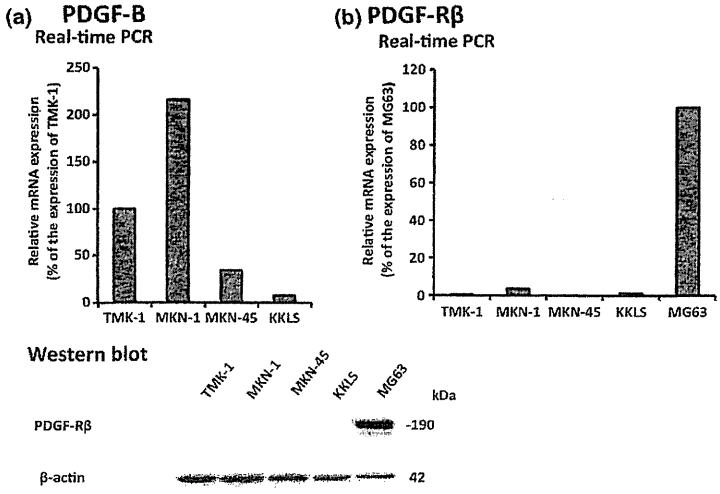

Fig. 1. Expression of platelet-derived growth factor B (PDGF-B) and PDGF receptor β (PDGF-Rβ) in gastric carcinoma cell lines. (a) Gastric cancer cell lines constitutively expressed mRNA for PDGF-B subunit at various levels. (b) PDGF-Rβ was not expressed by the cultured gastric carcinoma cell lines.

implantation of TMK-1 cells, mice ($n = 10$ each group) were randomly assigned to receive one of the following two treatments: daily oral gavage of water (control group) or daily oral gavage of imatinib (50 mg/kg, optimal biological dose as determined previously[17,24]). The treatments continued for 28 days. All therapy experiments were performed twice. The mice bearing orthotopic tumors were euthanized by methophane on day 29. For immunohistochemistry, the tumor tissues were fixed in formalin and embedded in paraffin.

Immunohistochemical determination of the area of lymphatic vessels. Paraffin-embedded tissues were used for immunohistochemical identification of Lyve-1. Sections were deparaffinized and rehydrated in PBS, microwaved in water for 5 min for antigen retrieval, incubated overnight at 4°C with mouse anti-Lyve-1 antibody, and incubated for 1 h at room temperature with a peroxidase-conjugated rat antimouse antibody. A positive reaction was detected by exposure to stable 3,3′-diaminobenzidine for 5–10 min. Slides were counterstained with Gill's hematoxylin. On slides immunolabeled for Lyve-1, only vessels with typical morphology (including a lumen) were counted as lymphatic vessels because of occasional weak antibody cross-reactivity with fibroblasts.[25] For quantification of the lymphatic vessel areas, 10 random fields at ×100 magnification were captured for each tumor, and the outline of each lymphatic vessel including a lumen was manually traced. The areas were then calculated with the use of NIH ImageJ software (http://rsbweb.nih.gov/ij/download.html).

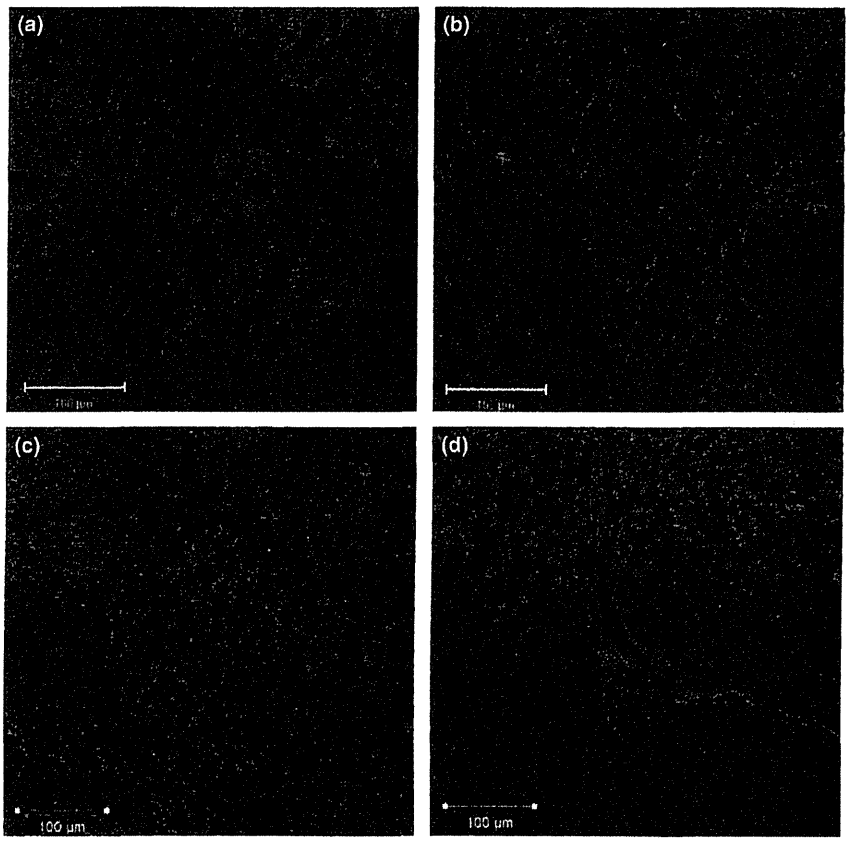

Fig. 2. Immunohistochemical detection of platelet-derived growth factor B (PDGF-B) and PDGF receptor β (PDGF-Rβ) in gastric carcinoma. (a,b) Immunolocalization of PDGF-B and PDGF-Rβ in human gastric carcinoma tissues. (c,d) Immunolocalization of PDGF-B and PDGF-Rβ in an orthotopic xenograft model (TMK-1 cell line). Expression of PDGF-B (a,c) and PDGF-Rβ (b,d) in tumor tissue appears red.

doi: 10.1111/j.1349-7006.2010.01639.x

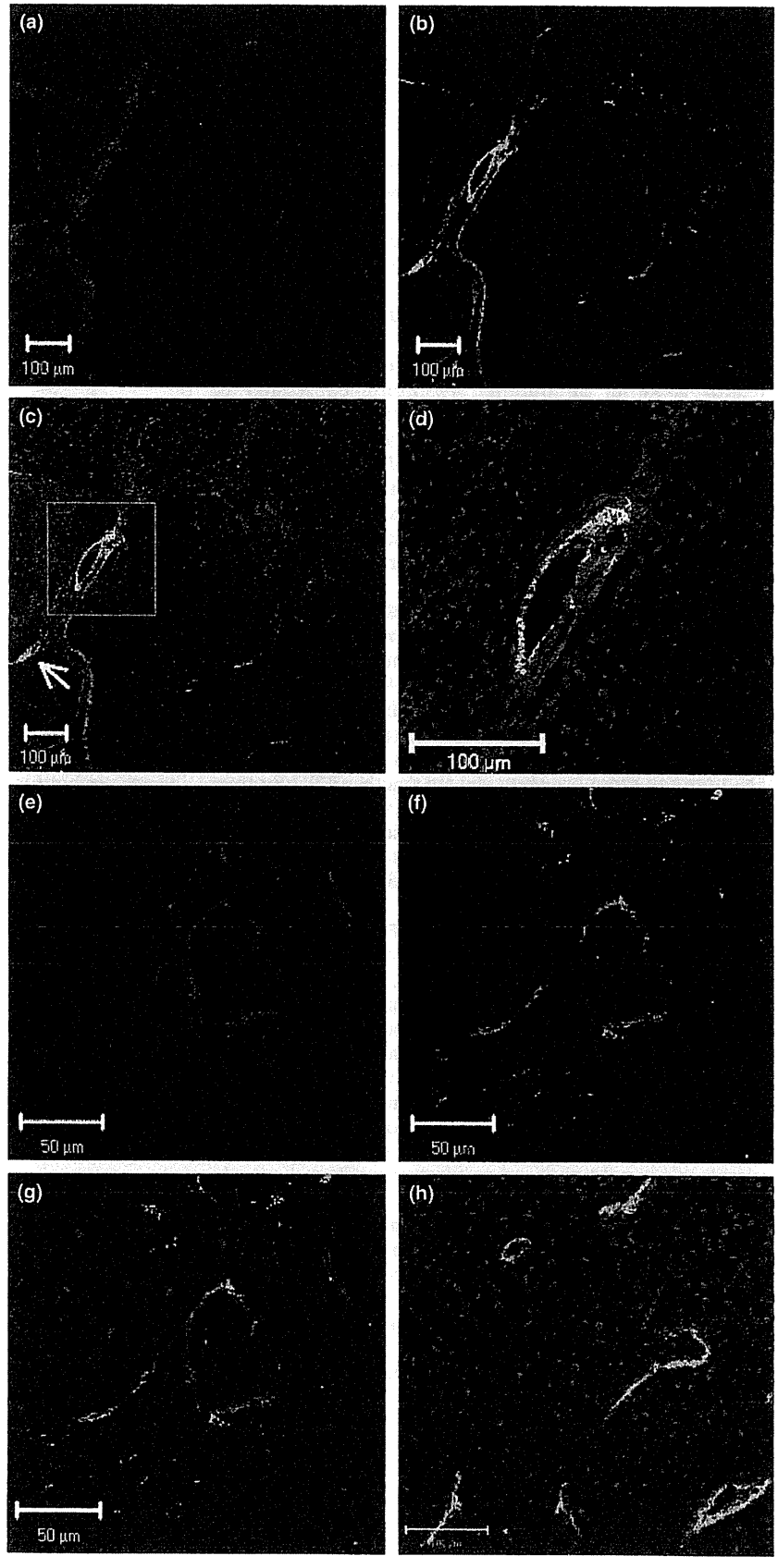

Fig. 3. Fluorescence double-labeled immunohistochemistry (IHC) of TMK-1 human gastric cancer cells growing in nude mice. Representative images show IHC for PDGF-Rβ in red and Lyve-1 (lymphatic endothelial marker) in green. (a–g) PDGF-Rβ was detected in lymphatic endothelial cells on enlarged and tortuous lymphatic vessels located immediately adjacent to tumor nests. Small lymphatic vessels (arrow) did not express PDGF-Rβ. (h) Intratumoral lymphatic vessels did not express PDGF-Rβ.

Statistical analysis. Results are expressed as mean ± SE. Wilcoxon/Kruskal–Wallis analysis was used to analyze between-group differences in continuous variables. A P-value of <0.05 was considered statistically significant.

Results

Expression levels of PDGF-B and PDGF-Rβ mRNAs in human gastric carcinoma. We initially examined mRNA expression of

PDGF-B and PDGF-Rβ by quantitative real-time PCR. The relative expression levels (T/N ratio) of PDGF-B and PDGF-Rβ are shown according to node status in Table 1. Patients with positive lymph nodes showed significantly greater expression of PDGF-B and PDGF-Rβ than node-negative patients ($P = 0.03$ and $P < 0.001$, respectively). We also examined the relation between PDGF-B and PDGF-Rβ mRNA expression and histologic type of human gastric carcinoma because diffuse-type gastric carcinoma is known to have abundant stroma and a high probability of lymph node metastasis. Expression of PDGF-B and PDGF-Rβ was significantly greater in patients with diffuse-type gastric carcinoma than in those with intestinal-type gastric carcinoma ($P = 0.03$ and $P = 0.004$, respectively) (Table 1).

Expression of PDGF-B and PDGF-Rβ in human gastric carcinoma cell lines growing in culture. We examined expression of PDGF-B and PDGF-Rβ in four human gastric carcinoma cell lines derived from different histological types. MG63 cells were used as a positive control for PDGF-R expression. The results of real-time PCR and western blot analysis are shown in Figure 1. Under culture conditions, expression of PDGF-B mRNA was found in all of the gastric cell lines, albeit at different levels. PDGF-Rβ was not expressed by the cultured gastric carcinoma cell lines.

Immunolocalization of PDGF-B and PDGF-Rβ in human gastric carcinoma tissues and in human gastric carcinoma cells growing in the mouse stomachs. We next confirmed PDGF-B and PDGF-Rβ expression *in vivo*. We used TMK-1 and KKLS cells for animal models because the other cell lines (MKN-1 and MKN-45) were difficult to grow in the mouse gastric walls. Representative photomicrographs are shown in Figure 2. Because TMK-1 tumors had more abundant stroma than KKLS tumors, it was convenient to use TMK-1 tumors to evaluate PDGF-B and PDGF-Rβ expression in stroma. In the surgical specimens and the orthotopic xenograft models, tumor cells expressed PDGF-B, but PDGF-Rβ was expressed predominantly by stromal cells (Fig. 2a–d).

Immunohistochemical analysis of PDGF-Rβ and Lyve-1 expression in TMK-1 tumors. To identify whether tumor-associated lymphatic vessels express PDGF-Rβ, we analysed co-localization of PDGF-Rβ and Lyve-1 (lymphatic endothelial cells). Co-localization of green (Lyve-1) and red (PDGF-Rβ) fluorescence appeared as yellow fluorescence, indicating that tumor-associated lymphatic vessels expressed PDGF-Rβ. PDGF-Rβ was expressed occasionally on lymphatic endothelial cells, especially on enlarged and tortuous lymphatic vessels located immediately adjacent to tumor nests (Fig. 3a–g). Lymphatic vessels in normal tissue or intratumoral lymphatic vessels did not express PDGF-Rβ (Fig. 3h).

Treatment of human gastric carcinoma growing in mouse stomachs. We determined the effects of imatinib, PDGF-Rβ thyrosine kinase inhibitor, on lymphatic vessels in tumors growing up from implantation of TMK-1 human gastric carcinoma cells into the stomachs of nude mice. The tumors treated with imatinib had reduced areas of lymphatic vessels in comparison to areas of lymphatic vessels in control tumors ($P < 0.05$) (Fig. 4).

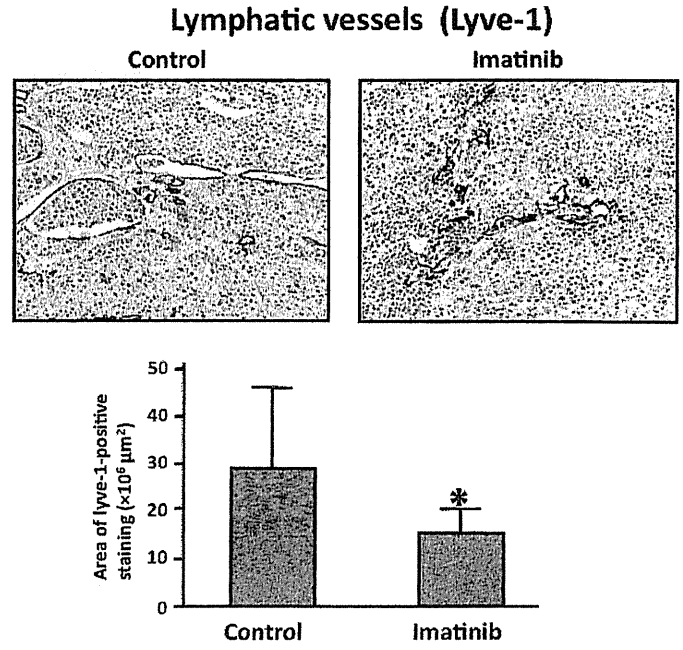

Fig. 4. Immunohistochemistry for Lyve-1 in TMK-1 orthotopic gastric tumors with and without imatinib treatment. Treatment with imatinib significantly reduced the area of lymphatic vessels. *$P < 0.05$; bars, SE.

Discussion

Lymph node metastasis is a common clinical finding in many human cancers and is associated with both aggressive disease and poor prognosis. Genetic and epigenetic alterations of tumor cells often lead to amplified expression of multiple growth factors that contribute to tumor growth, angiogenesis and lymphangiogenesis.[26]

VEGF-C and VEGF-D through interaction with VEGFR-3 expressed on lymphatic endothelial cells were once thought to be the only direct lymphangiogenic factors.[27] However, tumors with high lymphatic metastatic ability express additional growth factors at high levels, suggesting that these factors may contribute to tumor lymphangiogenesis.[26] In an extensive study in which Cao *et al.*[13] implanted PDGF-A and PDGF-B in mouse corneas, both factors were shown to induce growth of lymphatic vessels, although PDGF-B was more potent than PDGF-A. Additionally, its main receptor, PDGF-Rβ, was detected on the induced lymphatic endothelial cells. VEGF-C/-D and VEGFR-3 antagonists did not inhibit PDGF-B-induced lymphangiogenesis. PDGF-B was also shown to activate intracellular signaling components by phosphorylation of Akt, Src, and Erk. In the present study, patients with positive lymph nodes showed significantly greater expression of PDGF-B and PDGF-Rβ than that of node-negative patients.

Tumor blood vessels have been shown to differ morphologically from their normal counterparts. The endothelial cells are structurally and functionally abnormal and can acquire cytogenetic abnormalities while in the tumor microenvironment.[28] Tumor lymphatic vessels appear to be structurally disorganized, tortuous, and leaky.[13] These leaky tumoral lymphatics could provide a vulnerable structural basis for tumor cell invasion into the lymphatic system. Like tumor blood cells, tumor-associated lymphatic vessels have been recently shown to have differentially expressed genes. Clasper *et al.*[29] compared gene expression of purified lymphatic endothelial cells from highly metastatic fibrosarcoma and from dermal tissue. They found differential expression of some 792 genes that code for a variety of proteins including components of endothelial junctions, subendothelial matrix, and vessel growth/patterning. In our orthotopic gastric cancer model, Lyve-1-positive lymphatic vessels were shown to express PDGF-Rβ; not all lymphatic vessels expressed PDGF-Rβ. PDGF-Rβ was expressed occasionally on lymphatic endothelial cells, especially on enlarged and tortuous lymphatic vessels located immediately adjacent to tumor nests, whereas lymphatic vessels in normal tissue or intratumoral small lymphatic vessels did not express PDGF-Rβ. Additionally, we did not find PDGF-Rβ expression on lymphatic vessels of orthotopic tumors grown up from KKLS cells, which express

doi: 10.1111/j.1349-7006.2010.01639.x

low levels of PDGF-B (data not shown). In general, tumor cells in a neoplasm are biologically heterogeneous, and their phenotype can be modified by the organ microenvironment.[30] Our data indicate that tumor-associated lymphatic vessels are also biologically heterogeneous and that interplay between lymphatic vessels and tumor cells may have a more significant effect on the endothelial phenotype than previously anticipated. Additionally, blockade of PDGF-Rβ signaling by oral administration of the PDGF-R tyrosine kinase inhibitor imatinib significantly reduced the area of lymphatic vessels in our orthotopic mouse model of gastric cancer. In our experiment, lymph node metastasis was not inhibited by treatment with imatinib alone (control, 8/10 *vs* imatinib treatment, 7/10). To inhibit lymph node metastasis, reduction of the lymphatic vessel area seems to be insufficient. Combination therapy of imatinib with cytotoxic chemotherapeutic drugs may be needed to inhibit lymph node metastasis. Together, these findings indicate that PDGF-Rβ is preferentially expressed by activated, proliferating lymphatic endothelium but not by quiescent lymphatic vessels in normal tissue, a finding with important implications for the potential therapeutic use of targeted PDGF-Rβ-blocking strategies.

In conclusion, we found PDGF-B secreted by tumor cells and PDGF-Rβ expressed by stromal cells including lymphatic endothelial cells to be associated with lymphatic metastasis in gastric carcinoma. Thus, blockage of PDGF-induced lymphangiogenesis may be a reasonable approach to prevention and treatment of lymphatic metastasis.

Acknowledgments

This work was carried out with the kind cooperation of the Analysis Center of Life Science, Hiroshima University, Hiroshima, Japan, and we thank Novartis Pharma K.K. (Basel, Switzerland) for providing the imatinib used in the study. This work was supported, in part, by Grants-in-Aid for Cancer Research from the Ministry of Education, Culture, Science, Sports and Technology of Japan and from the Ministry of Health, Labor and Welfare of Japan.

Disclosure Statement

The authors have no conflict of interest.

References

1 Fidler IJ. The pathogenesis of cancer metastasis: the 'seed and soil' hypothesis revisited. *Nat Rev Cancer* 2003; **3**: 453–8.
2 Carmeliet P, Jain RK. Angiogenesis in cancer and other diseases. *Nature* 2000; **407**: 249–57.
3 Jussila L, Alitalo K. Vascular growth factors and lymphangiogenesis. *Physiol Rev* 2002; **82**: 673–700.
4 Karkkainen MJ, Haiko P, Sainio K *et al.* Vascular endothelial growth factor C is required for sprouting of the first lymphatic vessels from embryonic veins. *Nat Immunol* 2004; **5**: 74–80.
5 Makinen T, Jussila L, Veikkola T *et al.* Inhibition of lymphangiogenesis with resulting lymphedema in transgenic mice expressing soluble VEGF receptor-3. *Nat Med* 2001; **7**: 199–205.
6 Mandriota SJ, Jussila L, Jeltsch M *et al.* Vascular endothelial growth factor-C-mediated lymphangiogenesis promotes tumor metastasis. *EMBO J* 2001; **20**: 672–82.
7 Skobe M, Hawighorst T, Jackson DG *et al.* Induction of tumor lymphangiogenesis by VEGF-C promotes breast cancer metastasis. *Nat Med* 2001; **7**: 192–8.
8 Stacker SA, Achen MG, Jussila L, Baldwin ME, Alitalo K. Lymphangiogenesis and cancer metastasis. *Nat Rev Cancer* 2002; **2**: 573–83.
9 Kubo H, Cao R, Brakenhielm E, Makinen T, Cao Y, Alitalo K. Blockade of vascular endothelial growth factor receptor-3 signaling inhibits fibroblast growth factor-2-induced lymphangiogenesis in mouse cornea. *Proc Natl Acad Sci U S A* 2002; **99**: 8868–73.
10 Gale NW, Thurston G, Hackett SF *et al.* Angiopoietin-2 is required for postnatal angiogenesis and lymphatic patterning, and only the latter role is rescued by Angiopoietin-1. *Dev Cell* 2002; **3**: 411–23.
11 Kajiya K, Hirakawa S, Ma B, Drinnenberg I, Detmar M. Hepatocyte growth factor promotes lymphatic vessel formation and function. *EMBO J* 2005; **24**: 2885–95.
12 Hirakawa S, Kodama S, Kunstfeld R, Kajiya K, Brown LF, Detmar M. VEGF-A induces tumor and sentinel lymph node lymphangiogenesis and promotes lymphatic metastasis. *J Exp Med* 2005; **201**: 1089–99.
13 Cao R, Bjorndahl MA, Religa P *et al.* PDGF-BB induces intratumoral lymphangiogenesis and promotes lymphatic metastasis. *Cancer Cell* 2004; **6**: 333–45.
14 Pietras K, Sjoblom T, Rubin K, Heldin CH, Ostman A. PDGF receptors as cancer drug targets. *Cancer Cell* 2003; **3**: 439–43.
15 Heldin CH, Eriksson U, Ostman A. New members of the platelet-derived growth factor family of mitogens. *Arch Biochem Biophys* 2002; **398**: 284–90.
16 Li X, Eriksson U. Novel PDGF family members: PDGF-C and PDGF-D. *Cytokine Growth Factor Rev* 2003; **14**: 91–8.
17 Uehara H, Kim SJ, Karashima T *et al.* Effects of blocking platelet-derived growth factor-receptor signaling in a mouse model of experimental prostate cancer bone metastases. *J Natl Cancer Inst* 2003; **95**: 458–70.
18 Risau W, Drexler H, Mironov V *et al.* Platelet-derived growth factor is angiogenic in vivo. *Growth Factors* 1992; **7**: 261–6.
19 Ostman A. PDGF receptors-mediators of autocrine tumor growth and regulators of tumor vasculature and stroma. *Cytokine Growth Factor Rev* 2004; **15**: 275–86.
20 Pietras K. Increasing tumor uptake of anticancer drugs with imatinib. *Semin Oncol* 2004; **31**: 18–23.
21 Japanese Research Society for Gastric Cancer. *Japanese classification of gastric carcinoma*. Tokyo: Kanehara, 1999.
22 Druker BJ, Tamura S, Buchdunger E *et al.* Effects of a selective inhibitor of the Abl tyrosine kinase on the growth of Bcr-Abl positive cells. *Nat Med* 1996; **2**: 561–6.
23 Buchdunger E, Cioffi CL, Law N *et al.* Abl protein-tyrosine kinase inhibitor STI571 inhibits in vitro signal transduction mediated by c-kit and platelet-derived growth factor receptors. *J Pharmacol Exp Ther* 2000; **295**: 139–45.
24 Hwang RF, Yokoi K, Bucana CD *et al.* Inhibition of platelet-derived growth factor receptor phosphorylation by STI571 (Gleevec) reduces growth and metastasis of human pancreatic carcinoma in an orthotopic nude mouse model. *Clin Cancer Res* 2003; **9**: 6534–44.
25 Valencak J, Heere-Ress E, Kopp T, Schoppmann SF, Kittler H, Pehamberger H. Selective immunohistochemical staining shows significant prognostic influence of lymphatic and blood vessels in patients with malignant melanoma. *Eur J Cancer* 2004; **40**: 358–64.
26 Folkman J. Looking for a good endothelial address. *Cancer Cell* 2002; **1**: 113–5.
27 Alitalo K, Carmeliet P. Molecular mechanisms of lymphangiogenesis in health and disease. *Cancer Cell* 2002; **1**: 219–27.
28 Hida K, Hida Y, Amin DN *et al.* Tumor-associated endothelial cells with cytogenetic abnormalities. *Cancer Res* 2004; **64**: 8249–55.
29 Clasper S, Royston D, Baban D *et al.* A novel gene expression profile in lymphatics associated with tumor growth and nodal metastasis. *Cancer Res* 2008; **68**: 7293–303.
30 Fidler IJ, Poste G. The cellular heterogeneity of malignant neoplasms: implications for adjuvant chemotherapy. *Semin Oncol* 1985; **12**: 207–21.

UICC
global cancer control

IJC
International Journal of Cancer

Mesenchymal stem cells enhance growth and metastasis of colon cancer

Kei Shinagawa[1], Yasuhiko Kitadai[1], Miwako Tanaka[1], Tomonori Sumida[1], Michiyo Kodama[1], Yukihito Higashi[2], Shinji Tanaka[3], Wataru Yasui[4] and Kazuaki Chayama[1]

[1] Department of Medicine and Molecular Science, Graduate School of Biomedical Sciences, Hiroshima University, Hiroshima, Japan
[2] Department of Cardiovascular Physiology and Medicine, Graduate School of Biomedical Sciences, Hiroshima University, Hiroshima, Japan
[3] Department of Endoscopy, Hiroshima University Hospital, Hiroshima, Japan
[4] Department of Molecular Pathology, Graduate School of Biomedical Sciences, Hiroshima University, Hiroshima, Japan

Recently, mesenchymal stem cells (MSCs) were reported to migrate to tumor stroma as well as injured tissue. We examined the role of human MSCs in tumor stroma using an orthotopic nude mice model of KM12SM colon cancer. In *in vivo* experiments, systemically injected MSCs migrated to the stroma of orthotopic colon tumors and metastatic liver tumors. Orthotopic transplantation of KM12SM cells mixed with MSCs resulted in greater tumor weight than did transplantation of KM12SM cells alone. The survival rate was significantly lower in the mixed-cell group, and liver metastasis was seen only in this group. Moreover, tumors resulting from transplantation of mixed cells had a significantly higher proliferating cell nuclear antigen labeling index, significantly greater microvessel area and significantly lower apoptotic index. Splenic injection of KM12SM cells mixed with MSCs, in comparison to splenic injection of KM12SM cells alone, resulted in a significantly greater number of liver metastases. MSCs incorporated into the stroma of primary and metastatic tumors expressed α-smooth muscle actin and platelet-derived growth factor receptor-β as carcinoma-associated fibroblast (CAF) markers. In *in vitro* experiments, KM12SM cells recruited MSCs, and MSCs stimulated migration and invasion of tumor cells through the release of soluble factors. Collectively, MSCs migrate and differentiate into CAFs in tumor stroma, and they promote growth and metastasis of colon cancer by enhancing angiogenesis, migration and invasion and by inhibiting apoptosis of tumor cells.

Cancer Cell Biology

Mesenchymal stem cells (MSCs) are characterized by their ability to self-renew and differentiate into tissues of mesodermal origin, including bone, cartilage and adipose and connective tissues. Thus, they contribute to tissue regeneration.[1]

Key words: mesenchymal stem cells, carcinoma-associated fibroblasts, orthotopic colon cancer model, tumor microenvironment

Abbreviations: CAF: carcinoma-associated fibroblast; DAPI: 4′,6-diamidino-2-phenylindole; DMEM: Dulbecco's Modified Eagle's Medium; FACS: fluorescence-activated cell sorting; FAP: fibroblast activation protein; FBS: fetal bovine serum; FSP: fibroblast specific protein; HBSS: Hanks' balanced salt solution; MSC: mesenchymal stem cell; MVA: microvessel area; PBS: phosphate-buffered saline; PCNA: proliferating cell nuclear antigen; PCNA-LI: PCNA labeling index; PDGFR: platelet-derived growth factor receptor; SMA: smooth muscle actin; TUNEL: terminal deoxynucleotide transferase-mediated dUTP-biotin nick end labeling

Grant sponsors: Ministry of Education, Culture, Science, Sports and Technology of Japan (Grants-in-Aid for Cancer Research), Ministry of Health, Labor and Welfare of Japan

DOI: 10.1002/ijc.25440

History: Received 3 Jan 2010; Accepted 28 Apr 2010; Online 6 May 2010

Correspondence to: Yasuhiko Kitadai, Hiroshima University Graduate School of Biomedical Sciences, 1-2-3 Kasumi, Minami-ku, Hiroshima 734-8551, Japan, Tel.: +81-82-257-5191, Fax: +81-82-257-5194, E-mail: kitadai@hiroshima-u.ac.jp

MSCs are recruited from bone marrow to inflamed or damaged tissues by local endocrine signals, resulting in the formation of fibrous scars.[2,3] Tumor tissue contains abundant growth factors, cytokines and matrix-remodeling proteins, explaining why tumors are likened to wounds that never heal.[4] MSCs are reported to migrate to tumor sites as well as sites of injury and to incorporate into tumor stroma, but the effects of interactions between MSCs and tumor cells and the mechanisms underlying these effects remain unclear. Recent coinjection experiments revealed that MSCs promote tumor growth and metastasis.[5–13] Reports suggest that MSCs are involved in tumor invasion and angiogenesis,[5–7,14] immunosuppression[8,9] and inhibition of apoptosis.[11] Mishra *et al.* reported that MSCs can differentiate into carcinoma-associated fibroblast (CAF)-like cells by prolonged exposure to tumor-conditioned medium and that these cells promote tumor growth.[12,13] Theirs was the first report to show the relations between cancer cells, MSCs and CAFs in detail. Because accumulating evidence suggests that CAFs indeed promote the growth of tumors,[15–20] the hypothesis that CAFs originate from MSCs may have interesting clinical implications.

In most coinjection studies concerning the effect of MSCs on tumors, subcutaneous ectopic transplantation models were used, but these models are considered insufficient for examining tumor–stroma interactions.[21] The influence of the organ microenvironment on the biology of tumor cells has been recognized since Paget's "seed and soil" hypothesis,

which suggests that multiple interactions between tumor cells and specific organs determine whether metastasis will occur.[22] Organ-specific factors can influence the growth, vascularization, invasion and metastasis of human neoplasms.[23–25] Thus, we examined tumor–MSC interactions in the tumor microenvironment using a mouse orthotopic transplantation model of human colon cancer.

We found that circulating MSCs migrate not only to the orthotopic colon tumor but also to the metastatic liver tumors. In addition, we showed by coinjection study that MSCs promote the growth and metastasis of colon cancer and that MSCs incorporated into the tumor stroma express CAF markers. This is the first reported study to show the significance of tumor–MSC interactions in the growth and metastasis of colon cancer.

Material and Methods

Isolation and culture of human MSCs

MSCs were obtained from the iliac crest and plated in a dish with Dulbecco's Modified Eagle's Medium (DMEM) supplemented with 10% fetal bovine serum (FBS), L-glutamine and a penicillin–streptomycin mixture according to a protocol approved by the Ethics Committee of Hiroshima University Graduate School of Medicine, as described previously.[26] Nonadherent cells were removed after 72 hr, and adherent cells were detached from the plates and subcultured every 4–5 days in fresh medium supplemented with 1 ng/ml fibroblast growth factor-2.[27] Aliquots from passages 3–5 were frozen in liquid nitrogen for future use.

Characterization of human MSCs *in vitro*

In culture medium, MSCs formed a monolayer of adherent cells and looked like long spindle-shaped fibroblastic cells. The capacity for chondrogenic, adipogenic and osteogenic differentiation was confirmed with the use of a Human Mesenchymal Stem Cell Functional Identification Kit (R&D Systems, Minneapolis, MN). Cell surface antigens on these cells were analyzed by fluorescence-activated cell sorting, and we confirmed that the cells were positive for CD29, CD44, CD73, CD90, CD105, CD166 and MHC-DR, but negative for CD14, CD34 and Flk-1, as described previously.[26]

Colon cancer cell line and culture conditions

The human colon cancer cell line KM12SM[28,29] was kindly gifted by Dr. Isaiah J. Fidler (University of Texas). Cells were maintained in DMEM supplemented with 10% FBS, L-glutamine and a penicillin–streptomycin solution. The cultures were maintained for no longer than 12 weeks after recovery from frozen stock.

Animals and transplantation of tumor cells

Female athymic BALB/c nude mice were obtained from Charles River Japan (Tokyo, Japan). The mice were maintained under specific pathogen-free conditions and used when 8 weeks old. Study was carried out after permission was granted by the Committee on Animal Experimentation of Hiroshima University.

To produce cecal tumors, KM12SM cells in 50 μl of Hanks' balanced salt solution (HBSS) were injected into the cecal wall of nude mice under a dissecting microscope as described previously.[28] To produce experimental liver metastases, the cells were injected into the spleen of nude mice as described previously.[29]

Assessing migration of MSCs *in vivo*

To determine whether circulating MSCs have the ability to migrate to the orthotopic colon tumor, 1.0×10^6 KM12SM cells were transplanted into the cecal wall of three mice on day 0. Three weeks after tumor cell transplantation (on day 21), each mouse underwent injection of 1.0×10^6 PKH26 (Sigma)-labeled MSCs (in 200 μl of HBSS) into the tail vein. One week after this injection (on day 28), the mice were killed and necropsied.

To determine whether circulating MSCs also have the ability to migrate to the metastatic liver tumor, 0.5×10^6 KM12SM cells were transplanted into the spleen of three mice on day 0. One week after tumor cell transplantation (on day 7), each mouse underwent injection of 1.0×10^6 PKH26-labeled MSCs (in 200 μl of HBSS) into the tail vein. Three weeks after this injection (on day 28), the mice were killed.

Tumors were removed and stored in OCT Compound (Sakura Finetek Japan, Tokyo, Japan) and then snap-frozen in liquid nitrogen and stored at −80°C until tissue processing. Sections of PKH26-labeled tissues were analyzed by means of fluorescence confocal microscopy.

Examining the effect of MSCs on tumor growth in orthotopic colon tumors

To examine the effect of MSCs on tumor growth at the orthotopic site, coinjection studies were carried out. Mice were divided into three groups and underwent injection of (a) KM12SM cells alone (0.5×10^6, $n = 24$), (b) KM12SM cells mixed with MSCs [KM12SM:MSCs (0.5×10^6:1.0×10^6, ratio of 1:2, $n = 28$)], or (c) MSCs alone (1.0×10^6, $n = 10$).

Six weeks after intracecal transplantation of these cells, surviving mice were killed and necropsied [(a) $n = 21$, (b) $n = 12$, (c) $n = 10$]. Tumor weights, incidences of liver metastasis, and survival rates were evaluated. One part of the tumor tissue from each mouse was fixed in formalin-free IHC Zinc Fixative (PharMingen, San Diego, CA) and embedded in paraffin, and the other part was embedded in OCT Compound, rapidly frozen in liquid nitrogen and stored at −80°C.

Examining differentiation of MSCs commingled with tumor cells in orthotopic colon tumors

To evaluate whether commingled MSCs can differentiate into CAF-like cells, KM12SM cells mixed with PKH26-labeled MSCs (0.5×10^6:1.0×10^6, ratio of 1:2) were injected into the cecal wall of 3 mice. Three weeks after intracecal

transplantation, tumors were excised. Excised tumors were analyzed by means of fluorescence confocal microscopy to detect PKH26-labeled MSCs after immunofluorescence staining.

Assessing the effect of MSCs on liver metastasis and differentiation of MSCs in a liver metastasis model

To highlight the effect of MSCs on liver metastasis, we developed a model of liver metastasis by injecting tumor cells into mice spleen as described previously.[28,29] Mice were divided into two groups: (a) those injected with KM12SM cells alone (0.5×10^6, $n = 10$), and (b) those injected with KM12SM cells along with PKH26-labeled MSCs [KM12SM:PKH26-labeled MSCs (0.5×10^6:1.0×10^6, ratio of 1:2, $n = 10$)].

Four weeks after intrasplenic transplantation, tumor nodules on the liver surface were counted macroscopically. To examine whether MSCs can migrate from the primary site to the metastatic site and differentiate, metastatic tumors were analyzed by means of fluorescence confocal microscopy to detect PKH26-labeled MSCs after immunofluorescence staining.

Antibodies

The primary antibodies used were rabbit anti-platelet-derived growth factor receptor (PDGFR)-β (Santa Cruz Biotechnology, Santa Cruz, CA), rabbit anti-α-smooth muscle actin (SMA) (Abcam, Cambridge, UK), mouse anti-desmin (Molecular Probes, Eugene, OR), rabbit anti-fibroblast activation protein (FAP) (Abcam, Cambridge, UK), rabbit anti-fibroblast specific protein (FSP) (Abcam, Cambridge, UK), mouse anti- proliferating cell nuclear antigen (PCNA) (Dako, Glostrup, Denmark) and rat anti-mouse CD31 (BD Pharmingen, San Diego, CA). Biotinylated rabbit anti-rat IgG (Dako) and biotinylated goat anti-mouse IgG (Dako) were used as secondary antibodies. The fluorescent secondary antibody was Alexa Fluor® 488-labeled goat anti-rabbit IgG (Invitrogen, Carlsbad, CA).

Immunohistochemical determination of PCNA, apoptotic cells and microvessel area (MVA)

Paraffin-embedded tissues cut into 4-μm sections and frozen tissues cut into 8-μm sections were used for immunohistochemical identification of PCNA and CD31, respectively. Immunohistochemistry was performed as described previously.[30] The PCNA labeling index (PCNA-LI) was expressed as the ratio of positively stained tumor cells to the total tumor cells, given as a percentage for each case. Ten random areas without necrosis in a section were selected by light microscopy; at least 2,000 cells were counted under 400× magnification. Apoptotic cells in frozen sections of KM12SM tumors were detected by terminal deoxynucleotide transferase-mediated dUTP-biotin nick end labeling (TUNEL method) with the ApopTag Plus Peroxidase *In Situ* Apoptosis Detection Kit (Chemicon, Temecula, CA) according to the manufacturer's instructions. The apoptotic index (AI) was expressed as the ratio of positively stained tumor cells and apoptotic bodies to all tumor cells, given as a percentage for each case. Twenty random areas without necrosis in a section were selected by light microscopy; at least 5,000 cells were counted under 400× magnification. Angiogenic activity was evaluated according to the areas of microvessels stained with anti-mouse CD31 antibody. For quantification of the MVA, ten random fields at 100× magnification were captured for each tumor, and the outline of each microvessel including a lumen was manually traced. The area was then calculated with the use of NIH ImageJ software.

Immunofluorescence staining

Frozen specimens cut into 8-μm sections or cells cultured on slide glass were fixed for 15 min in 4% paraformaldehyde in phosphate-buffered saline (PBS). The slides were blocked briefly in protein blocking solution, incubated overnight at 4°C with the Fab fragment of anti-mouse IgG to block endogenous immunoglobulins if necessary, and incubated overnight at 4°C with anti-α-SMA (1:400), anti-FAP (1:100), anti-FSP (1:100), anti-desmin (1:400) or anti-PDGFR-β (1:400). The slides were washed with PBS and then incubated for 1 hr at room temperature with Alexa Fluor® 488-labeled secondary antibody (1:600). Nuclear counterstain with 4′,6-diamidino-2-phenylindole (DAPI) was applied for 10 min, and mounting medium was placed on each specimen with a glass coverslip. α-SMA-, FAP-, FSP-, desmin- or PDGFR-β-positive cells were identified by green fluorescence, whereas PKH26 on MSCs was identified by red fluorescence. Colocalization of PKH26 and α-SMA, FAP, FSP, desmin or PDGFR-β was detected by yellow staining.

Confocal microscopy

Confocal fluorescence images were captured with a 20× or 40× objective lens on a Zeiss LSM 510 laser scanning microscopy system (Carl Zeiss, Thornwood, NY) equipped with a motorized Axioplan microscope, argon laser (458/477/488/514 nm, 30 mW), HeNe laser (543 nm, 1 mW), HeNe laser (633 nm, 5 mW), LSM 510 control and image acquisition software and appropriate filters (Chroma Technology Corp., Brattleboro, VT). Confocal images were exported to Adobe Photoshop software, and image montages were prepared.

Collection of conditioned medium

To detect any paracrine effects of MSCs on KM12SM cells, conditioned medium from MSCs was collected and used for subsequent study. In detail, 1.0×10^6 MSCs were seeded in a 100-mm plate, and 48 hr later, 20 ml of DMEM with 0.5% FBS was added for 24-hr incubation. The medium was then collected, sterile filtered, aliquoted and stored at −20°C until use. DMEM with 0.5% FBS was used as control medium.

Proliferation assay

The proliferative effect of MSC-conditioned medium on KM12SM cells was analyzed. KM12SM (4.0×10^4) cells were

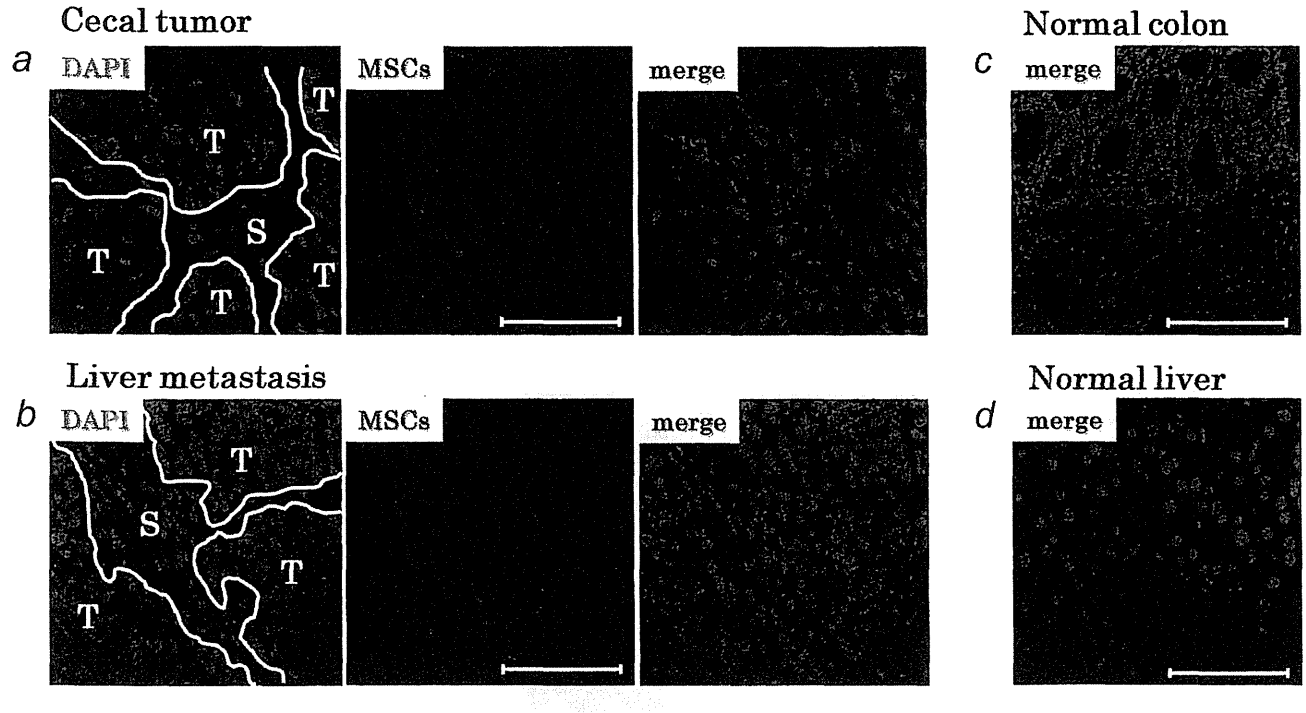

Figure 1. Migration of circulating MSCs to the stromata of orthotopic colon tumor and metastatic liver tumor. Systemically administered MSCs possess the ability to migrate to the orthotopic colon tumor stroma (*a*) and metastatic liver tumor (*b*). 4′,6-Diamidino-2-phenylindole (DAPI) staining for cell nuclei (blue) shows the outline of the stroma within tumor tissue. PKH26-labeled MSCs (red) are detected specifically in the tumor stroma but not in the noncancerous tissues, such as normal colon and normal liver (*c* and *d*). T: tumor nest; S: stroma; Scale bars: 100 μm.

seeded in a 12-well plate, and the next day, control medium or MSC-conditioned medium was added (day 0). The medium was changed on days 2 and 4, and the number of cells was counted on days 2, 4 and 7 ($n = 6$ in each group).

Migration assay

The migratory ability of KM12SM cells was assayed with the use of a 12-well microchamber plate with uncoated inserts (12-μm pore size, Corning Costar, Tokyo, Japan). Either 1.0×10^5 MSCs in DMEM with 0.5% FBS or the medium alone was plated into the lower chambers. After 24 hr of incubation at 37°C, upper chambers containing 1.0×10^5 KM12SM cells in DMEM with 0.5% FBS were set into the lower chambers. Three wells were used for each experiment. After 48 hr of incubation at 37°C, inserts were fixed with 10% buffered formalin solution and stained with hematoxylin. The cells on the upper surface of the membranes were removed with cotton swabs. The number of migrating cells was counted in three random fields per filter at 200× magnification.

The migratory ability of MSCs was also assayed by means of a 24-well microchamber plate with uncoated inserts (8-μm pore size, Corning Costar). Either 2.0×10^4 KM12SM in DMEM with 0.5% FBS or medium alone was plated into the lower chambers. After 4 hr of incubation at 37°C, upper chambers containing 2.0×10^4 MSCs in DMEM with 0.5% FBS were set into the lower chambers. Three wells were used for each experiment. After 16 hr of incubation at 37°C, inserts were fixed with 10% buffered formalin solution and stained with hematoxylin. The number of migrating cells was determined as described above.

Invasion assay

The invasive ability of KM12SM cells was assayed by using a 24-well microchamber plate (12 μm pore size, Corning Costar) according to a previously described method,[31] but with minor modifications. In brief, the upper surface of each membrane was coated with Matrigel (240 μg per filter, BD Biosciences, San Jose, CA). KM12SM (1.0×10^5) cells were seeded in the upper chamber with serum free medium, and MSC-conditioned medium or control medium was added to the lower chambers. Three wells were used for each experiment. After 46 hr of incubation at 37°C, inserts were treated as in the migration assay. The number of invading cells was counted in three random fields per filter at 100× magnification.

Statistical analysis

Survival curves were drawn by the Kaplan and Meier method, and the log rank test was used to analyze differences in survival rates. Student's or Welch's *t*-test or the Wilcoxon test was used to analyze differences in other variables, as appropriate. Data are expressed as mean ± standard error

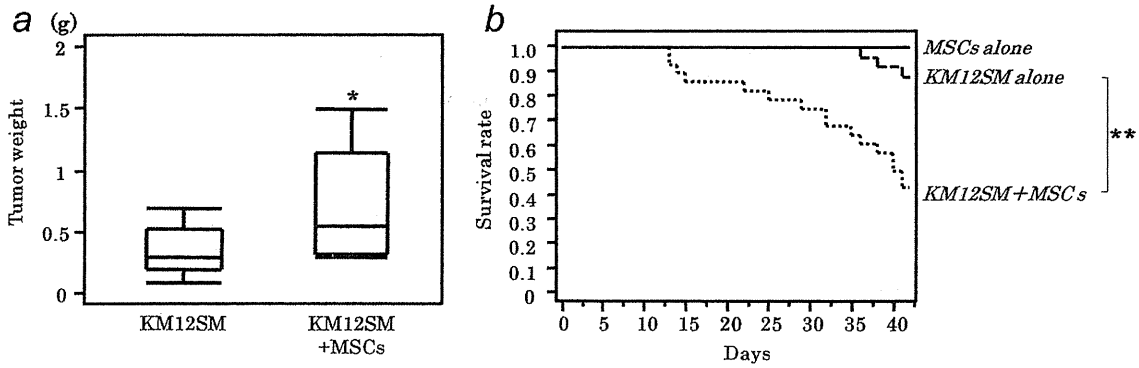

c

Liver metastasis \ Transplanted cells	KM12SM alone	KM12SM +MSCs
+	0	2
—	21	10
Total number of mice	21	12

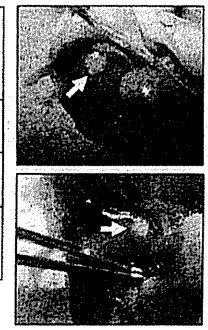

Figure 2. (*a*) Transplantation of KM12SM cells mixed with MSCs (0.5×10^6:1.0×10^6, $n = 12$ mice) resulted in significantly greater tumor weight than that resulting from transplantation of KM12SM cells alone (0.5×10^6, $n = 21$). *$p < 0.05$, Bars: SE. (*b*) Kaplan–Meier curves show survival of mice bearing KM12SM cells alone ($n = 24$), KM12SM cells mixed with MSCs ($n = 28$) and MSCs alone ($n = 10$). The survival rate was significantly lower in the mixed-cell group. p values were determined by log-rank test. **$p < 0.001$. (*c*) Macroscopic liver metastasis was seen only in the group that received KM12SM cells mixed with MSCs. Arrows denote macroscopic liver metastases.

(SE). Probability values of <0.05 were considered significant. All statistical analyses were performed with JMP software (SAS Institute, Cary, NC).

Results

Migration of MSCs to the stroma of orthotopic primary tumors and to metastatic liver tumors

After injection of PKH-labeled MSCs into the tail veins of tumor-bearing mice, MSCs were detected specifically in the tumor stroma (Fig. 1*a*) at the primary site. MSCs were also detected in the stroma of metastatic liver tumors (Fig. 1*b*). In contrast, MSCs were not detected in the noncancerous tissues, such as normal colonic mucosa and liver (Figs. 1*c* and 1*d*).

Promotion of the growth of orthotopic colon tumors by MSCs

At 6 weeks after transplantation of KM12SM cells alone, KM12SM cells mixed with MSCs, or MSCs alone into the cecal wall of nude mice, the weight of tumors resulting from mixed cells was significantly greater than the weight of tumors resulting from tumor cells alone (0.47 ± 0.10 *vs.* 1.03 ± 0.38 g, $p < 0.05$; Fig. 2*a*). The survival rate was significantly lower in the mixed-cell group than in the group that received KM12SM cells alone ($p < 0.001$; Fig. 2*b*). MSCs alone did not have the ability to generate any tumor and did not affect the survival of mice. Surviving mice were killed on day 42. Liver metastasis was not seen macroscopically in the 21 mice that received tumor cells alone, but liver metastasis was seen macroscopically in two of the 12 mice in the mixed-cell group (Fig. 2*c*). To clarify the mechanisms underlying the growth-promoting effect, we examined proliferation, apoptosis and angiogenesis in primary tumors by immunohistochemistry. The PCNA-LI, AI and MVA were compared between the tumors resulting from transplantation of KM12SM cells alone and those resulting from transplantation of KM12SM cells mixed with MSCs. The PCNA-LI was significantly higher (42.0 ± 5.3 *vs.* 62.9 ± 4.6 %, $p < 0.05$; Fig. 3*a*) and the AI was significantly lower in the mixed-cell group (7.0 ± 0.6 *vs.* 3.4 ± 0.3 %, $p < 0.001$; Fig. 3*b*). The MVA was significantly greater in the tumors from the mixed-cell group (13,719 ± 2,154 *vs.* 24,594 ± 2,230 μm^2, $p < 0.01$; Fig. 3*c*).

Differentiation of MSCs in orthotopic colon tumors

Three weeks after transplantation of KM12SM cells mixed with PKH26-labeled MSCs, commingled MSCs were incorporated into the tumor stroma and expressed α-SMA, PDGFR-β, desmin, FSP and FAP as CAF markers (Fig. 4*a*), but they did not express human CD31 (data not shown). The

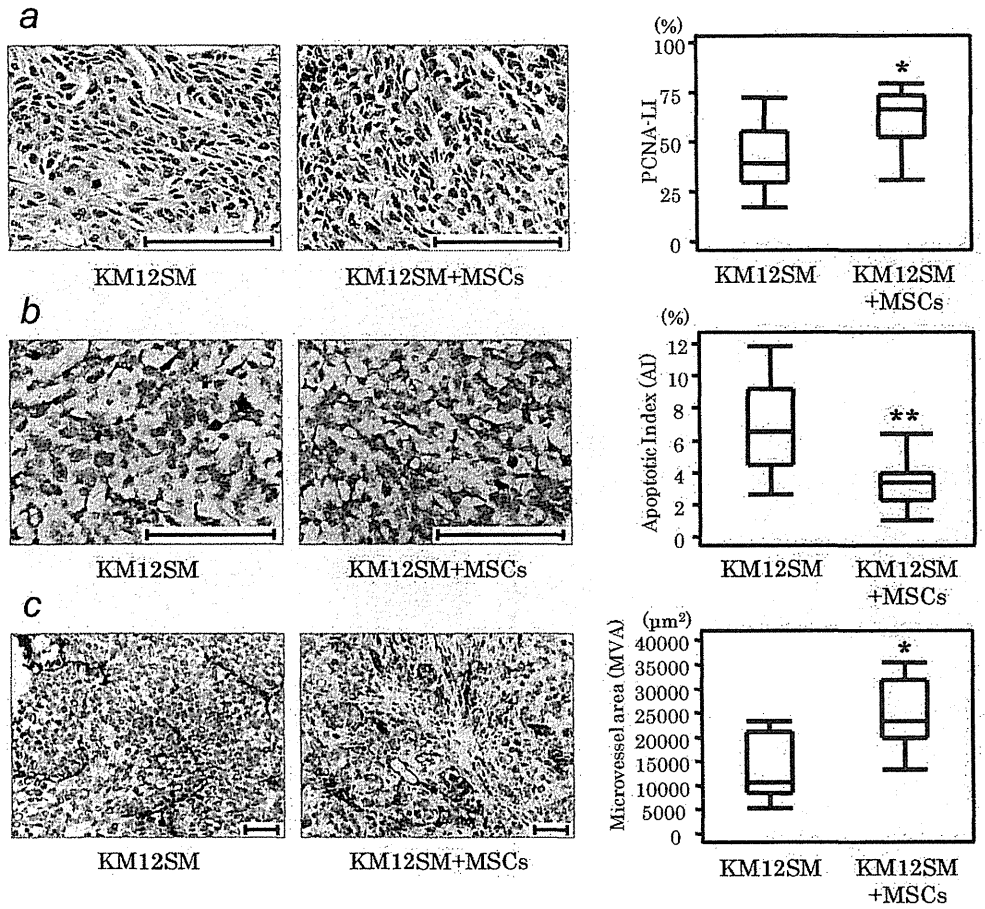

Figure 3. MSCs enhance proliferation and angiogenesis and inhibit apoptosis *in vivo*. (*a*) Proliferative activity was evaluated by the proliferating cell nuclear antigen labeling index (PCNA-LI, %). The PCNA-LI was significantly higher in tumors from the mixed-cell group than in tumors from the group that received KM12SM cells alone. (*b*) Apoptotic cells in tumors were detected by the terminal deoxynucleotide transferase-mediated dUTP-biotin nick end labeling method, and the apoptotic index (AI, %) was calculated. The AI was significantly lower in tumors from the mixed-cell group than in tumors from the group that received KM12SM cells alone. (*c*) Tumor microvessel areas (MVAs) were calculated. The MVA was significantly greater in tumors from the mixed-cell group. *$p < 0.01$, Bars: SE. **$p < 0.001$, Bars: SE. Scale bars: 100 μm

morphology and distribution of MSCs within tumor stroma were similar to those of CAFs. Before the introduction of MSCs into mice, we examined the expression of α-SMA and PDGFR-β in MSCs during *in vitro* propagation. MSCs expressed PDGFR-β at a low level but not α-SMA (Fig. 4*b*).

Increase in the number of liver metastases by injection of KM12SM cells mixed with MSCs

Transplantation of KM12SM cells mixed with MSCs into the spleen of nude mice resulted in a significantly greater number of liver metastases at 4 weeks than that resulting from transplantation of KM12SM cells alone (2.6 ± 4.3 *vs.* 15.1 ± 6.0, $p < 0.01$; Fig. 5*a*). In addition, commingled MSCs migrated to the stroma of metastatic liver tumors and expressed α-SMA, PDGFR-β, desmin, FAP and FSP as CAF markers (Fig. 5*b*).

Attraction between KM12SM cells and MSCs *in vitro*

To investigate whether KM12SM cells have the ability to attract MSCs *in vitro*, migration assay was performed. We found that more human MSCs migrated toward the KM12SM cell culture than toward the medium without KM12SM cells (30.9 ± 3.5 *vs.* 24.2 ± 3.6 cells/field, $p < 0.05$; Fig. 6*a*).

We then examined the effects of MSCs on migration and invasion of KM12SM cells. The ability of KM12SM cells to migrate toward the MSC culture was significantly greater than the ability of these cells to migrate toward the medium without MSCs (114.9 ± 16.1 *vs.* 170.2 ± 18.5 cells/field, $p < 0.05$; Fig. 6*b*). Moreover, the invasive ability of KM12SM cells was significantly greater toward MSC-conditioned medium than toward control medium (33.1 ± 7.4 *vs.* 59.0 ± 7.9 cells/field, $p < 0.05$; Fig. 6*c*).

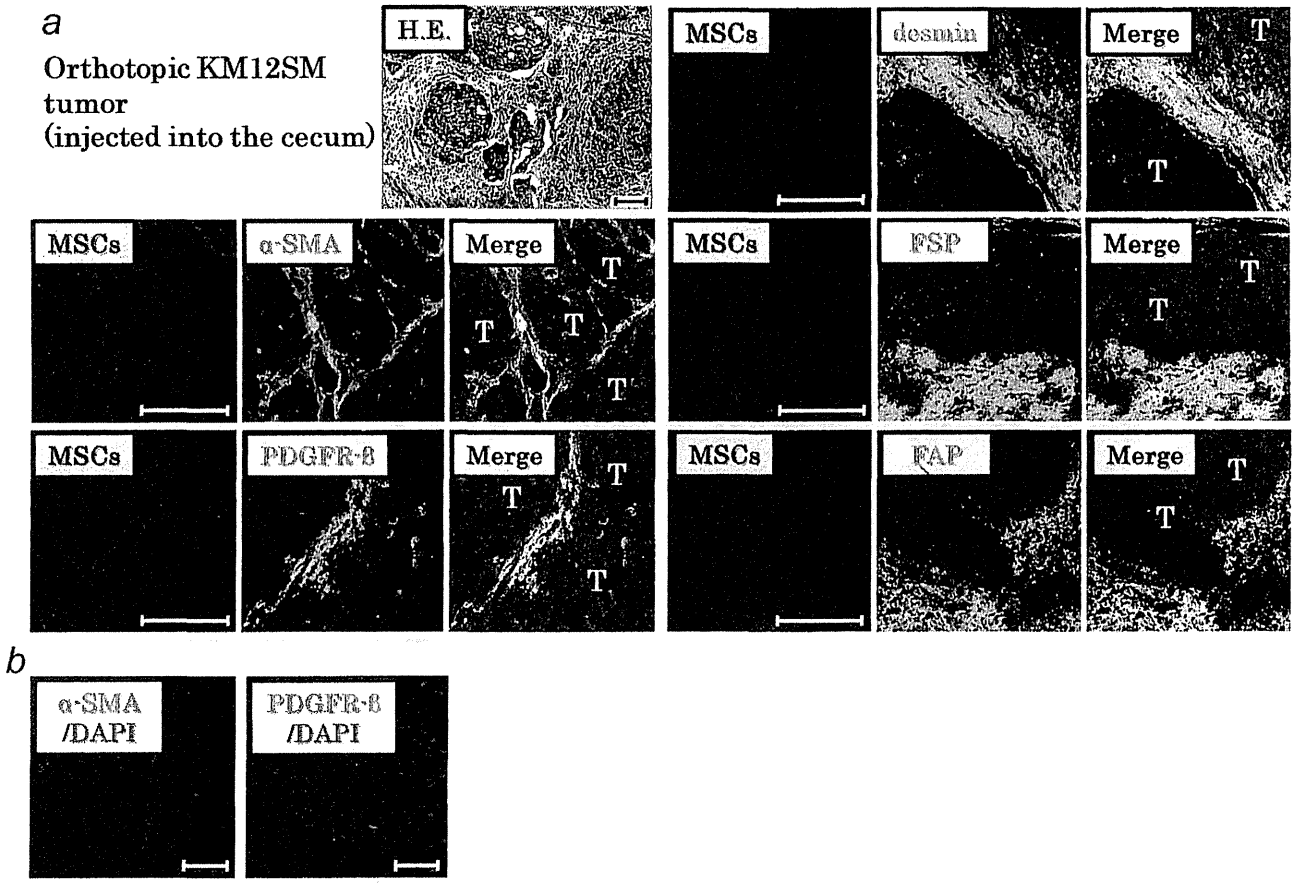

Figure 4. (*a*) Immunofluorescence staining for α-SMA, PDGFR-β, desmin, FSP or FAP (green) was performed in the orthotopic colon tumors resulting from KM12SM cells mixed with PKH26-labeled MSCs (red). Commingled MSCs were incorporated into the tumor stroma and expressed α-SMA, PDGFR-β, desmin, FSP and FAP. (*b*) Immunofluorescence staining for α-SMA and PDGFR-β was performed in MSCs cultured on slide glass. There was no α-SMA expression and low PDGFR-B expression in the cultured MSCs. T: tumor nest; Scale bars: 100 μm

The effect of the soluble factors secreted from MSCs on the proliferation of KM12SM cells was also examined. KM12SM cells were exposed to control medium or MSC-conditioned medium and then counted on days 2, 4 and 7. No significant difference was observed in the number of KM12SM cells between the two groups at any time point (Fig. 6*d*).

Discussion

It has been reported that MSCs migrate to a variety of tumors, such as melanomas,[32,33] gliomas[34,35] and colon,[14,36] pancreatic[37,38] and breast cancers.[10,33,39,40] Studies have implicated molecules such as CXCL12 (SDF-1)/CXCR4,[36] CCL2 (MCP-1)/CCR2[39] and PDGF[37] in the tumor-homing ability of MSCs. In the present study, we showed that circulating MSCs have the ability to migrate not only to the stroma of orthotopic colon tumors but also to metastatic lesions. In *in vitro* experiments, we observed that tumor cells recruit MSCs through the release of soluble factors. Although the exact molecular mechanisms that govern MSC migration are not fully characterized, this migratory ability points to MSCs as attractive candidates for delivery vehicles of antitumor agents.[32–35] However, several coinjection experiments have revealed that MSCs promote tumor growth and metastasis,[5–13] which would present a serious obstacle to using MSCs as delivery vehicles for anti-cancer therapy. Thus, the precise effects of MSCs on tumor growth and progression and the mechanism underlying these effects should be elucidated.

We previously reported that expression of metastasis-related genes by cancer cells and stromal cells is higher in orthotopic (cecal wall) KM12SM human colon carcinomas than in ectopic (subcutaneous) tumors.[15,16,25] The stromal reaction and metastatic potential are increased in the orthotopic microenvironment. Therefore, orthotopic models should be used to study tumor–stroma or tumor–MSC interaction.[21,23,41,42] In our study, orthotopic transplantation of tumor cells mixed with MSCs into the cecal wall, in comparison to orthotopic transplantation of tumor cells alone, resulted in significantly greater tumor weight. In primary tumors, PCNA-LI (proliferation) and MVA (angiogenesis)

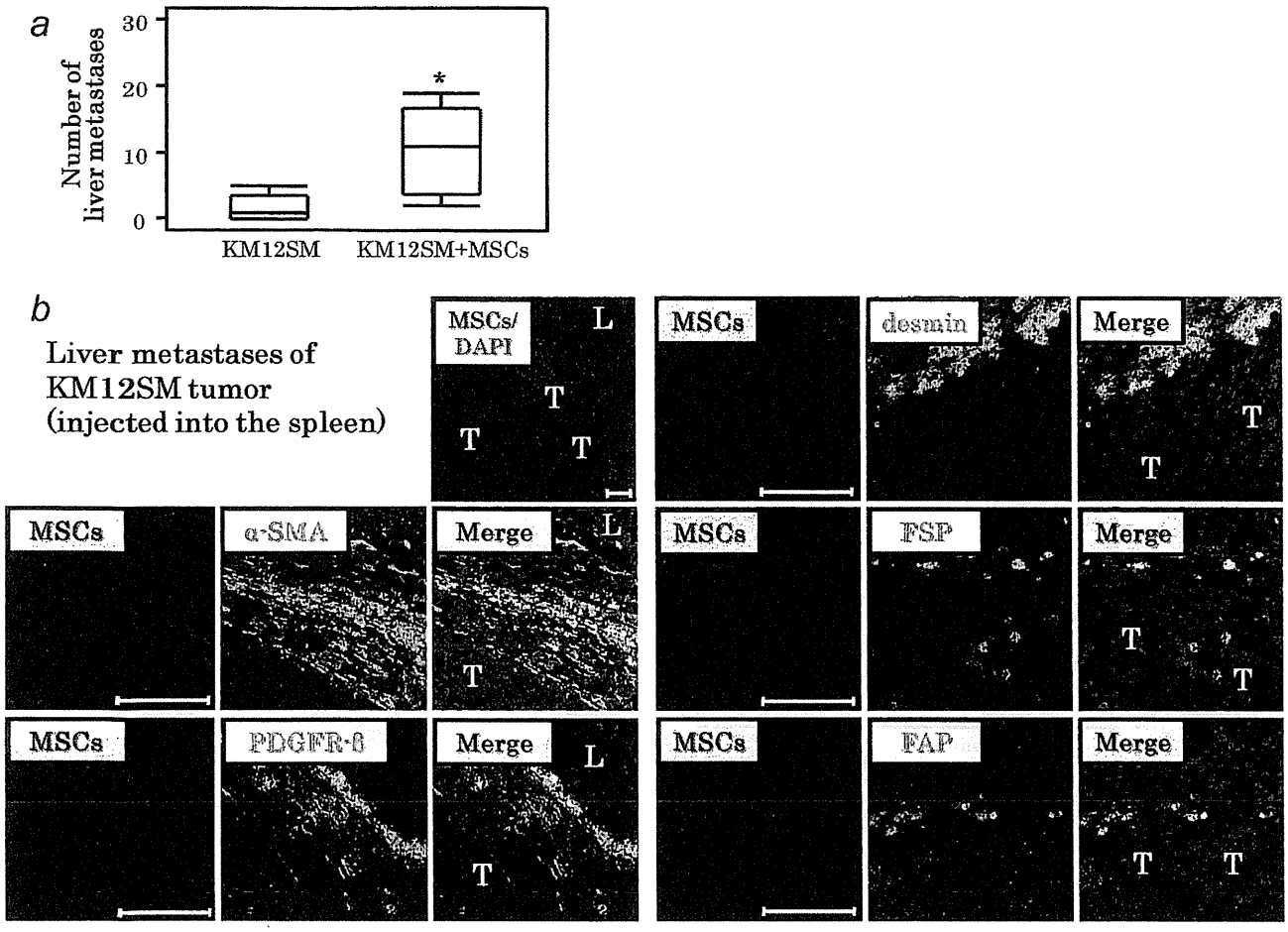

Figure 5. (*a*) Transplantation of KM12SM cells mixed with MSCs (0.5×10^6:1.0×10^6, $n = 10$) resulted in a significantly greater number of liver metastases than the number resulting from transplantation of KM12SM cells alone (0.5×10^6, $n = 10$). *$p < 0.01$, Bars: SE. (*b*) Immunofluorescence staining for α-SMA, PDGFR-β, desmin, FSP and FAP (green) was performed in metastatic liver tumors resulting from KM12SM cells mixed with PKH26-labeled MSCs (red) injected into the spleen. Commingled MSCs migrated to the stroma of metastatic liver tumors and expressed α-SMA, PDGFR-β, desmin, FSP and FAP. L: normal liver, T: tumor nest; Scale bars: 100 μm.

were significantly increased, and the AI (apoptosis) was significantly lower in the tumors from the mixed-cell group. More intriguingly, macroscopic liver metastasis appeared only in the mixed-cell group, and the survival rate was significantly lower in this group. MSCs promoted migration and invasion of KM12SM cells *in vitro*. Because MSCs enhance proliferation, angiogenesis, migration and invasion and inhibit apoptosis of tumor cells, they may promote tumor growth and metastasis, which are followed by decreased survival. These findings are consistent with previously reported findings.[6,7,11]

In addition, we found commingled MSCs were functionally incorporated into the stroma of orthotopic colon tumors, where they expressed α-SMA, PDGFR-β, desmin, FAP and FSP as CAF markers. These results appear to corroborate the *in vitro* findings of Mishra *et al.*, who showed that MSCs exposed to tumor-conditioned medium for 30 days can act as CAF-like cells.[12,13] CAFs are known to promote tumor growth and metastasis, and phenotypes of CAFs are distinct from those of normal fibroblasts.[43,44] CAFs may arise from fibroblasts residing in local tissues,[18] periadventitial cells including pericytes and vascular smooth muscle cells,[45] endothelial cells[46] or bone marrow–derived cells including various stem cells.[47] MSCs differentiate by nature into tissues of mesodermal origin, so it is reasonable to suppose that CAFs derive from MSCs.

To more specifically determine the effect of MSCs on metastasis *in vivo*, we used an experimental liver metastasis model, and we found that MSCs enhanced the metastatic potential of KM12SM cells. The number of liver metastases was increased by coimplantation with MSCs; thus, MSCs may affect colonization step and maintain cancer cells. MSCs commingled with tumor cells at the primary tumor site (spleen) were able to travel to the stroma of metastatic foci in the liver, where they expressed CAF markers. These findings indicate that MSCs support tumor metastasis not only at the primary site but also at metastatic sites.

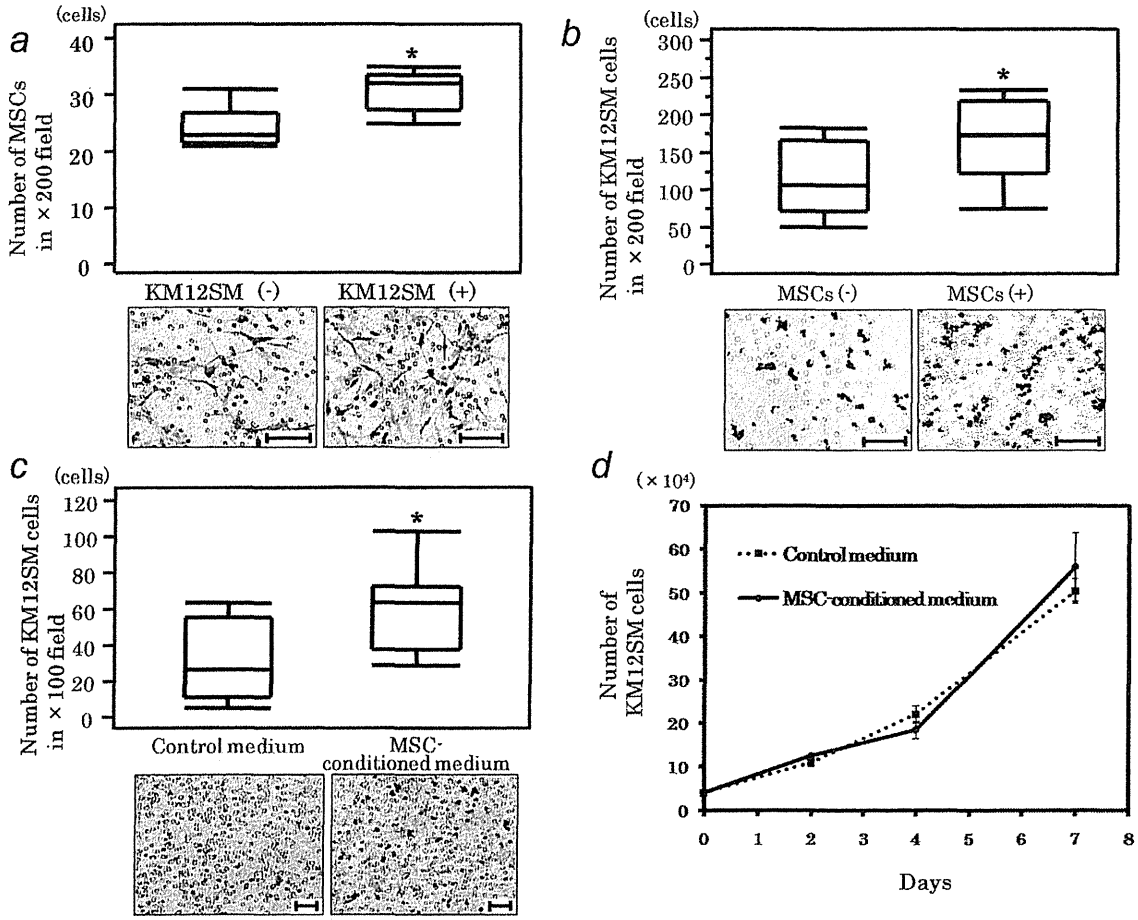

Figure 6. Interactions between KM12SM cells and MSCs *in vitro*. (*a*) The migratory ability of MSCs was analyzed by transwell assay. A significantly greater number of MSCs migrated toward the culture of KM12SM cells than toward the medium without KM12SM cells. (*b*) The migratory ability of KM12SM cells was also stimulated by coculture with MSCs. KM12SM cells were plated into upper chambers, which were then set into the lower chambers with or without MSCs. More KM12SM cells migrated toward the culture of MSCs than toward the medium without MSCs. (*c*) Effect of MSCs on the invasion of KM12SM cells. KM12SM cells were seeded in the upper chambers with serum free medium, and MSC-conditioned medium or control medium was added to the lower chambers. More KM12SM cells invaded Matrigel toward MSC-conditioned medium than toward control medium. Lower panels are typical photographs of the assay. $*p < 0.05$, Bars: SE. Scale bars: 100 μm. (*d*) Proliferation curves. KM12SM cells were exposed to control medium or MSC-conditioned medium and then counted on days 2, 4 and 7. No significant difference was observed in the number of cells between groups at any time point.

Karnoub *et al.* reported that CCL5 secreted from MSCs acts on the CCR5 of breast cancer cells only at the primary site and temporarily promotes lung metastasis without influencing primary tumor growth and neoangiogenesis[10]; in fact, MSCs did not exist at the sites of lung metastasis. They speculated that the enhanced metastatic ability was due to enhanced extravasation and colonization of cancer cells at the metastatic site. They also showed that MSCs promoted lung metastasis of all breast cancer cell lines used in their study, but the growth kinetics of MSC-containing tumors at the primary sites differ between each breast cancer cell line. Thus, differences in experimental conditions, such as the kinds of cell lines and the sites (ectopic or orthotopic) of transplantation, may influence growth and angiogenesis of the primary tumors.

Our data indicate that MSCs may directly encourage tumor cells at the primary site to metastasize to the liver and that metastasized tumor cells may in turn recruit MSCs to metastatic sites where the MSCs differentiate into supporting CAF-like cells. Understanding the molecular mechanisms of interaction between tumor cells and MSCs could lead to establishment of new therapies for targeting tumor stroma at both primary and metastatic sites. Orthotopic transplantation models should be used in *in vivo* studies of tumor–MSC interactions for the design of anticancer therapies.

Acknowledgements

The authors thank Ms. Megumi Wakisaka, Mr. Shinichi Norimura, and Ms. Emiko Hisamoto for their excellent technical assistance. This work was carried out with the kind cooperation of the Analysis Center of Life Science, Hiroshima University (Hiroshima, Japan).

References

1. Pittenger MF, Mackay AM, Beck SC, Jaiswal RK, Douglas R, Mosca JD, Moorman MA, Simonetti DW, Craig S, Marshak DR. Multilineage potential of adult human mesenchymal stem cells. *Science* 1999;284:143–7.
2. Fox JM, Chamberlain G, Ashton BA, Middleton J. Recent advances into the understanding of mesenchymal stem cell trafficking. *Br J Haematol* 2007;137: 491–502.
3. Gregory CA, Prockop DJ, Spees JL. Non-hematopoietic bone marrow stem cells: molecular control of expansion and differentiation. *Exp Cell Res* 2005;306: 330–5.
4. Dvorak HF. Tumors: wounds that do not heal. Similarities between tumor stroma generation and wound healing. *N Engl J Med* 1986;315:1650–9.
5. Sun B, Zhang S, Ni C, Zhang D, Liu Y, Zhang W, Zhao X, Zhao C, Shi M. Correlation between melanoma angiogenesis and the mesenchymal stem cells and endothelial progenitor cells derived from bone marrow. *Stem Cells Dev* 2005;14:292–8.
6. Zhu W, Xu W, Jiang R, Qian H, Chen M, Hu J, Cao W, Han C, Chen Y. Mesenchymal stem cells derived from bone marrow favor tumor cell growth in vivo. *Exp Mol Pathol* 2006;80:267–74.
7. Annabi B, Naud E, Lee YT, Eliopoulos N, Galipeau J. Vascular progenitors derived from murine bone marrow stromal cells are regulated by fibroblast growth factor and are avidly recruited by vascularizing tumors. *J Cell Biochem* 2004;91:1146–58.
8. Djouad F, Bony C, Apparailly F, Louis-Plence P, Jorgensen C, Noel D. Earlier onset of syngeneic tumors in the presence of mesenchymal stem cells. *Transplantation* 2006;82:1060–6.
9. Djouad F, Plence P, Bony C, Tropel P, Apparailly F, Sany J, Noel D, Jorgensen C. Immunosuppressive effect of mesenchymal stem cells favors tumor growth in allogeneic animals. *Blood* 2003;102: 3837–44.
10. Karnoub AE, Dash AB, Vo AP, Sullivan A, Brooks MW, Bell GW, Richardson AL, Polyak K, Tubo R, Weinberg RA. Mesenchymal stem cells within tumour stroma promote breast cancer metastasis. *Nature* 2007;449:557–63.
11. Ramasamy R, Lam EW, Soeiro I, Tisato V, Bonnet D, Dazzi F. Mesenchymal stem cells inhibit proliferation and apoptosis of tumor cells: impact on in vivo tumor growth. *Leukemia* 2007;21:304–10.
12. Mishra PJ, Mishra PJ, Humeniuk R, Medina DJ, Alexe G, Mesirov JP, Ganesan S, Glod JW, Banerjee D. Carcinoma-associated fibroblast-like differentiation of human mesenchymal stem cells. *Cancer Res* 2008;68:4331–9.
13. Mishra PJ, Mishra PJ, Glod JW, Banerjee D. Mesenchymal stem cells: flip side of the coin. *Cancer Res* 2009;69:1255–8.
14. Hung SC, Deng WP, Yang WK, Liu RS, Lee CC, Su TC, Lin RJ, Yang DM, Chang CW, Chen WH, Wei HJ, Gelovani JG. Mesenchymal stem cell targeting of microscopic tumors and tumor stroma development monitored by noninvasive in vivo positron emission tomography imaging. *Clin Cancer Res* 2005;11:7749–56.
15. Kitadai Y, Sasaki T, Kuwai T, Nakamura T, Bucana CD, Fidler IJ. Targeting the expression of platelet-derived growth factor receptor by reactive stroma inhibits growth and metastasis of human colon carcinoma. *Am J Pathol* 2006;169:2054–65.
16. Kitadai Y, Sasaki T, Kuwai T, Nakamura T, Bucana CD, Hamilton SR, Fidler IJ. Expression of activated platelet-derived growth factor receptor in stromal cells of human colon carcinomas is associated with metastatic potential. *Int J Cancer* 2006;119: 2567–74.
17. Orimo A, Gupta PB, Sgroi DC, Arenzana-Seisdedos F, Delaunay T, Naeem R, Carey VJ, Richardson AL, Weinberg RA. Stromal fibroblasts present in invasive human breast carcinomas promote tumor growth and angiogenesis through elevated SDF-1/ CXCL12 secretion. *Cell* 2005;121:335–48.
18. De Wever O, Mareel M. Role of tissue stroma in cancer cell invasion. *J Pathol* 2003;200:429–47.
19. Lieubeau B, Garrigue L, Barbieux I, Meflah K, Gregoire M. The role of transforming growth factor beta 1 in the fibroblastic reaction associated with rat colorectal tumor development. *Cancer Res* 1994;54: 6526–32.
20. Hu M, Polyak K. Microenvironmental regulation of cancer development. *Curr Opin Genet Dev* 2008;18:27–34.
21. Hurst DR, Welch DR. A MSC-ing link in metastasis? *Nat Med* 2007;13:1289–91.
22. Paget S. The distribution of secondary growths in cancer of the breast. *Cancer Metastasis Rev* 1989;8:98–101.
23. Fidler IJ. Critical factors in the biology of human cancer metastasis: twenty-eighth G.H.A. Clowes memorial award lecture. *Cancer Res* 1990;50:6130–8.
24. Fidler IJ, Poste G. The cellular heterogeneity of malignant neoplasms: implications for adjuvant chemotherapy. *Semin Oncol* 1985;12:207–21.
25. Kitadai Y, Bucana CD, Ellis LM, Anzai H, Tahara E, Fidler IJ. In situ mRNA hybridization technique for analysis of metastasis-related genes in human colon carcinoma cells. *Am J Pathol* 1995;147: 1238–47.
26. Ishii M, Koike C, Igarashi A, Yamanaka K, Pan H, Higashi Y, Kawaguchi H, Sugiyama M, Kamata N, Iwata T, Matsubara T, Nakamura K, et al. Molecular markers distinguish bone marrow mesenchymal stem cells from fibroblasts. *Biochem Biophys Res Commun* 2005;332:297–303.
27. Tsutsumi S, Shimazu A, Miyazaki K, Pan H, Koike C, Yoshida E, Takagishi K, Kato Y. Retention of multilineage differentiation potential of mesenchymal cells during proliferation in response to FGF. *Biochem Biophys Res Commun* 2001;288:413–9.
28. Morikawa K, Walker SM, Jessup JM, Fidler IJ. In vivo selection of highly metastatic cells from surgical specimens of different primary human colon carcinomas implanted into nude mice. *Cancer Res* 1988;48:1943–8.
29. Morikawa K, Walker SM, Nakajima M, Pathak S, Jessup JM, Fidler IJ. Influence of organ environment on the growth, selection, and metastasis of human colon carcinoma cells in nude mice. *Cancer Res* 1988;48:6863–71.
30. Hwang RF, Yokoi K, Bucana CD, Tsan R, Killion JJ, Evans DB, Fidler IJ. Inhibition of platelet-derived growth factor receptor phosphorylation by STI571 (Gleevec) reduces growth and metastasis of human pancreatic carcinoma in an orthotopic nude mouse model. *Clin Cancer Res* 2003;9:6534–44.
31. Repesh LA. A new in vitro assay for quantitating tumor cell invasion. *Invasion Metastasis* 1989;9:192–208.
32. Studeny M, Marini FC, Champlin RE, Zompetta C, Fidler IJ, Andreeff M. Bone marrow-derived mesenchymal stem cells as vehicles for interferon-beta delivery into tumors. *Cancer Res* 2002;62:3603–8.
33. Chen X, Lin X, Zhao J, Shi W, Zhang H, Wang Y, Kan B, Du L, Wang B, Wei Y, Liu Y, Zhao X. A tumor-selective biotherapy with prolonged impact on established metastases based on cytokine gene-engineered MSCs. *Mol Ther* 2008;16:749–56.
34. Nakamizo A, Marini F, Amano T, Khan A, Studeny M, Gumin J, Chen J, Hentschel S, Vecil G, Dembinski J, Andreeff M, Lang FF. Human bone marrow-derived mesenchymal stem cells in the treatment of gliomas. *Cancer Res* 2005;65:3307–18.
35. Nakamura K, Ito Y, Kawano Y, Kurozumi K, Kobune M, Tsuda H, Bizen A, Honmou O, Niitsu Y, Hamada H. Antitumor effect of genetically engineered mesenchymal stem cells in a rat glioma model. *Gene Ther* 2004;11:1155–64.
36. Menon LG, Picinich S, Koneru R, Gao H, Lin SY, Koneru M, Mayer-Kuckuk P, Glod J, Banerjee D. Differential gene expression